Asymptotic and numerical modelling of flows in fractured porous media

Philippe Angot, Franck Boyer, Florence Hubert

ASYMPTOTIC AND NUMERICAL MODELLING OF FLOWS IN FRACTURED POROUS MEDIA

Philippe ANGOT, Franck BOYER and Florence HUBERT[1]

Abstract. This study concerns some asymptotic models used to compute the flow outside and inside fractures in a porous medium. The flow is governed by the Darcy law both in the fractures and in the porous matrix with large discontinuities in the permeability tensor. These fractures are supposed to have a small thickness with respect to the macroscopic length scale, so that we can asymptotically reduce them to immersed polygonal fault interfaces and the model finally consists in a coupling between a d-dimensional elliptic problem and a (d-1)-dimensional one on the sharp interfaces modelling the fractures.

A cell-centered finite volume scheme on general polygonal meshes fitting the interfaces is derived to solve the set of equations with the additional differential transmission conditions linking both pressure and normal velocity jumps through the interfaces. We prove the convergence of the FV scheme for any set of data and parameters of the models and derive existence and uniqueness of the solution to the asymptotic models proposed. The models are then numerically experimented for fully or partially immersed fractures. Some numerical results are reported showing different kinds of flows in the case of impermeable or partially/fully permeable fractures. The influence of the variation of the aperture of the fractures is also investigated. The numerical solutions of the asymptotic models are validated by comparing them to the solution of the global Darcy model or to some analytic solutions.

1991 Mathematics Subject Classification. 76S05 - 74S10 - 35J25 - 35J20 - 65N15.

The dates will be set by the publisher.

1. Introduction

The present work addresses the numerical modelling of flows in fractured porous media by means of finite volume methods. The flow in the fracture domain Ω_f, in general fully immersed in the porous matrix Ω, is assumed to be governed by the Darcy law, as in the porous matrix, with an anisotropic permeability tensor $\mathbf{K}_f$. Our objective is to study asymptotic "double-permeability" models of fracture flow interacting with the matrix flow where the fractures are reduced to sharp interfaces Σ when the fracture aperture b_f is going to zero. More precisely, if l_m and l_p denote respectively the macroscopic and pores length scales, we have : $l_p \ll b_f \ll l_m$. The models involve some algebraic or differential immersed transmission conditions on the mean fracture surface Σ which combine the jumps of both pressure and normal velocity through the fault interface. The fractures may be "impermeable" (no jump of normal velocity with jumps of pressure on Σ), "fully permeable" (jumps of normal velocity with no jump of pressure on Σ), or characteristic of intermediate cases according to some

Keywords and phrases: Fractured porous media, Darcy flow, Finite volume method, Asymptotic models of flow.

[1] Université de Provence and CNRS, Laboratoire d'Analyse Topologie et Probabilités
39 rue F. Joliot Curie, F-13453 Marseille cedex 13.

Email : [angot,fboyer,fhubert]@cmi.univ-mrs.fr

physical phenomena altering their properties with time : mechanical effects (erosion, sedimentation, clogging, thermomechanical stress), chemical effects... [7, 14].

The global Darcy simulations of such problems require refined meshes inside the fracture domain Ω_f, that are usually very expensive. Hence the asymptotic models, where the fractures are reduced to immersed polygonal fault interfaces, are useful to provide a good approximation of the global flow at a lower cost.

Outline

The paper is organized as follows. Section 2 is devoted to the derivation of the asymptotic models of flow in fractured porous media we are interested in. The permeability anisotropy along the curvilinear coordinates associated with Σ is taken into account. The models depend on quadrature rules used to approximate the mean variables across the fracture and are characterized by a real parameter $\xi \geq \frac{1}{2}$.

We state and prove in Section 3 the global solvability of the asymptotic models in the case of a fully immersed fracture inside the porous matrix. In Section 4, a cell-centered finite volume scheme is proposed to approximate the solution of this problem. We prove the convergence of the finite volume approximate solution towards the unique solution of the asymptotic model under study, for any value of the parameter $\xi \in [\frac{1}{2}, +\infty[$.

Numerical investigations of the validity of the asymptotic models is proposed in Section 5. All the numerical results of the asymptotic models are compared to the solutions of the global double-permeability Darcy system, discretized by means of a *modified Discrete Duality Finite Volume* scheme on meshes locally refined in the neighborhood of the fractures. Such m-DDFV schemes are proved to be first-order in the discrete H^1- norm in [9], for any kind of anisotropy and heterogeneity of the permeability tensor.

We first illustrate the various typical flows we can expect depending on the physical properties of the fracture (impermeable, permeable, ...) in the case of a single fracture and we study the influence of the choice of the quadrature parameter ξ.

Then, the behavior of the model and some of its limits are illustrated on more complex situations: a fracture network, a non-constant aperture fracture. Finally we compare our result with analytical solutions obtained in [19] in the case of a lens-shaped fracture in an infinite porous matrix.

2. Asymptotic models of flow in fractured porous media

We consider an open polygonal bounded domain $\tilde{\Omega} \subset \mathbb{R}^d$ ($d = 2$ or 3 in practice); $\Gamma \stackrel{\text{def}}{=} \partial\tilde{\Omega}$ is divided into two disjoint subsets $\Gamma = \overline{\Gamma}_D \cup \overline{\Gamma}_N$, $\Gamma_D \cap \Gamma_N = \emptyset$, on which Dirichlet or Neumann boundary conditions will be respectively considered. For sake of simplicity, we concentrate now on the 2D case, see Fig. 1. There is no difficulty to consider numerous disjoint fractures or fractures in contact with the boundary of the domain but we only treat here the case of a single fully immersed 1D polygonal fracture $\Sigma \subset \tilde{\Omega}$.

Let us define the open bounded set $\Omega \subset \tilde{\Omega}$, representing the porous matrix, such that $\tilde{\Omega} = \Omega \cup \Sigma$ and its boundary $\partial\Omega = \Gamma \cup \Sigma$. It is always possible to embed Σ within a polygonal interface $\tilde{\Sigma} \supset \Sigma$ which divides the domain $\tilde{\Omega}$ into two open disjoint subdomains Ω^- and Ω^+ such that $\tilde{\Omega} = \Omega^- \cup \tilde{\Sigma} \cup \Omega^+$. Let $\mathbf{n}$ be the outward unit normal vector on Γ, and $\boldsymbol{\nu}$ the unit normal vector on Σ oriented from Ω^- to Ω^+. The outward unit normal to $\partial\Omega^+$ on Σ is then $\mathbf{n}^+ = -\boldsymbol{\nu}$ and the outward unit normal to $\partial\Omega^-$ on Σ is $\mathbf{n}^- = \boldsymbol{\nu}$. Let $\boldsymbol{\tau}$ be a unit tangential vector on Σ so that $(\boldsymbol{\tau}, \boldsymbol{\nu})$ is positively oriented, and s a normalized curvilinear coordinate parametrizing Σ in the direction given by $\boldsymbol{\tau}$. In our bidimensional situation, the boundary of Σ is composed by two points $\partial\Sigma = \{\partial\Sigma^+, \partial\Sigma^-\}$ defined in such a way that $s = 0$ in $\partial\Sigma^-$ and $s = |\Sigma|$ in $\partial\Sigma^+$.

For any function ψ in $H^1(\Omega)$, let $\gamma^+\psi$ and $\gamma^-\psi$ be the traces of ψ on each side of Σ, $\overline{\psi} = \frac{1}{2}(\gamma^+\psi + \gamma^-\psi)$ the arithmetic mean of traces of ψ, and $[\![\psi]\!] = (\gamma^+\psi - \gamma^-\psi)$ the jump of traces of ψ on Σ oriented by $\boldsymbol{\nu}$ (see Section 3.1.1). Let $\nabla_{\boldsymbol{\tau}}$ and $\nabla_{\boldsymbol{\tau}}\cdot$ denote the tangential gradient and divergence operators along Σ.

Notice that the sets Ω^+ and Ω^- will never appear neither in the final set of equations nor in the finite volume scheme we will propose. They are only introduced to fix an orientation and to give a precise meaning of the trace operators γ^+ and γ^-.

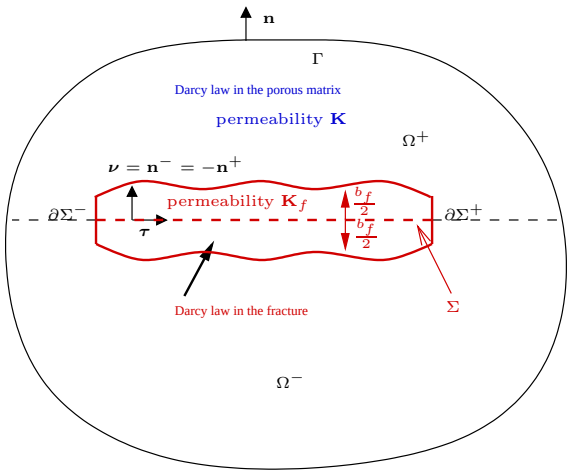

FIGURE 1. Configuration for "'double-permeability" models.

2.1. **Governing equations for the flow in the porous matrix**

We suppose that the flow in the porous matrix Ω is governed by a mass conservation equation together with Darcy's law relating the gradient of the pressure p to the filtration velocity $\mathbf{v}^p$ and some usual boundary conditions on Γ, see Fig. 1 :

$$\begin{aligned} \nabla \cdot \mathbf{v}^p &= Q \text{ in } \Omega & (1)\\ \mathbf{v}^p &= -\frac{1}{\mu}\mathbf{K}\cdot(\nabla p - \rho\mathbf{g}) \text{ in } \Omega & (2)\\ p &= p^D \text{ on } \Gamma_D & (3)\\ \mathbf{v}^p\cdot\mathbf{n} &= 0 \text{ on } \Gamma_N & (4) \end{aligned}$$

where $\mathbf{K}$ is the permeability tensor of the porous medium, symmetric and positive definite, $\mu > 0$ and $\rho > 0$ the dynamic viscosity and the density of the fluid, $\mathbf{g}$ the gravity, and Q a mass source term. It is of course possible to consider more general boundary conditions on Γ_N like non-homogeneous Fourier boundary conditions for instance but we focus our attention here on homogeneous neumann conditions.

2.2. **Asymptotic model of flow in the fracture**

2.2.1. *Averaging the Darcy law across the fracture*

The flow inside the fracture domain $\Omega_f = \left\{ s + t\boldsymbol{\nu}(s) \,/\, s \in \Sigma,\, t \in \left[-\frac{b_f(s)}{2}, \frac{b_f(s)}{2}\right] \right\}$ with $b_f \ll 1$, is supposed to satisfy the Darcy law for a permeability tensor $\mathbf{K}_f$ given in the curvilinear frame $(\boldsymbol{\tau}, \boldsymbol{\nu})$ by

$$\mathbf{K}_f = \begin{bmatrix} \mathbf{K}_{f,\boldsymbol{\tau}} & 0 \\ 0 & \mathbf{K}_{f,\boldsymbol{\nu}} \end{bmatrix},$$

that is $(\mathbf{K}_f\boldsymbol{\tau},\boldsymbol{\tau}) = \mathbf{K}_{f,\boldsymbol{\tau}}$, $(\mathbf{K}_f\boldsymbol{\nu},\boldsymbol{\nu}) = \mathbf{K}_{f,\boldsymbol{\nu}}$. Note that we assume that $\mathbf{K}_f$ is diagonal in the curvilinear frame, that is $(\mathbf{K}_f\boldsymbol{\tau},\boldsymbol{\nu}) = 0$. It is possible to write down a model for general permeabilities such that $(\mathbf{K}_f\boldsymbol{\tau},\boldsymbol{\nu}) \neq 0$ but its analysis is then much more intricate.

The coefficients $\mathbf{K}_{f,\boldsymbol{\tau}}$ and $\mathbf{K}_{f,\boldsymbol{\nu}}$ can be estimated by specific studies of flows inside different kinds of fractures [1]. Transversely to Σ, the variations of the permeability $\mathbf{K}_f$ in the fracture are neglected and we define the

mean quantities of the variables :

$$\mathbf{u}_{f,\boldsymbol{\tau}} = \frac{1}{b_f}\int_{-\frac{b_f}{2}}^{\frac{b_f}{2}} \mathbf{v}^p \cdot \boldsymbol{\tau}\, dt,\ \mathbf{u}_{f,\boldsymbol{\nu}} = \frac{1}{b_f}\int_{-\frac{b_f}{2}}^{\frac{b_f}{2}} \mathbf{v}^p \cdot \boldsymbol{\nu}\, dt,\ \Pi_f p = \frac{1}{b_f}\int_{-\frac{b_f}{2}}^{\frac{b_f}{2}} p\, dt,\ Q_f = \frac{1}{b_f}\int_{-\frac{b_f}{2}}^{\frac{b_f}{2}} Q\, dt.$$

First, we average the mass conservation equation (1) and the Darcy law (2) over the cross-section of the fracture which gives respectively :

$$\begin{aligned}
\nabla_{\boldsymbol{\tau}} \cdot (b_f \mathbf{u}_{f,\boldsymbol{\tau}}) + [\![\mathbf{v}^p \cdot \boldsymbol{\nu}]\!] &= b_f Q_f, \\
\mathbf{u}_{f,\boldsymbol{\tau}} &= -\frac{1}{\mu}\mathbf{K}_{f,\boldsymbol{\tau}}(\nabla_{\boldsymbol{\tau}}\Pi_f p - \rho\, \mathbf{g}\cdot\boldsymbol{\tau}), \\
\mathbf{u}_{f,\boldsymbol{\nu}} &= -\frac{1}{\mu}\mathbf{K}_{f,\boldsymbol{\nu}}\left(\frac{[\![p]\!]}{b_f} - \rho \mathbf{g}\cdot\boldsymbol{\nu}\right).
\end{aligned}$$

Then, by using the trapezoidal quadrature rule to approximate the mean variables with an error in $\mathcal{O}(b_f^2)$, *i.e.*

$$\Pi_f p \simeq \overline{p}, \quad \mathbf{u}_{f,\boldsymbol{\nu}} \simeq \overline{\mathbf{v}^p \cdot \boldsymbol{\nu}}, \tag{5}$$

we get the first asymptotic model of flow along the fault interface Σ :

$$\begin{aligned}
\nabla_{\boldsymbol{\tau}} \cdot (b_f \mathbf{u}_{f,\boldsymbol{\tau}}) &= b_f Q_f - [\![\mathbf{v}^p \cdot \boldsymbol{\nu}]\!] \text{ in } \Sigma && (6)\\
\mathbf{u}_{f,\boldsymbol{\tau}} &= -\frac{1}{\mu}\mathbf{K}_{f,\boldsymbol{\tau}}(\nabla_{\boldsymbol{\tau}}\Pi_f p - \rho\, \mathbf{g}\cdot\boldsymbol{\tau}),\ \text{in } \Sigma && (7)\\
\Pi_f p &= \overline{p},\ \text{in } \Sigma, && (8)\\
\overline{\mathbf{v}^p \cdot \boldsymbol{\nu}} &= -\frac{1}{\mu}\mathbf{K}_{f,\boldsymbol{\nu}}\left(\frac{[\![p]\!]}{b_f} - \rho \mathbf{g}\cdot\boldsymbol{\nu}\right) \text{ in } \Sigma. && (9)
\end{aligned}$$

Finally, a natural Neumann boundary condition for the pressure on $\partial\Sigma$ is added to close the system :

$$\mathbf{u}_{f,\boldsymbol{\tau}} = 0 \quad \text{ on } \partial\Sigma.$$

This boundary condition states that, since the fracture aperture is small, most of the fluid exchanges takes place through the boundary of the fracture. Other kind of boundary conditions can of course be considered : in the case where the fracture is touching Γ it can be natural to impose a Dirichlet boundary condition on the pressure on $\partial\Sigma$ (see some numerical results in Section 5).

2.2.2. *Generalization for other quadrature rules*

Such models have already been proposed in [13, 17]. In fact, in those references other quadrature rules are used in place of the trapezoidal rule to approximate the cross-section mean values of the pressure $\Pi_f p$ and of $\mathbf{v}^p \cdot \boldsymbol{\nu}$ in (5). Following the computations in the above references, we propose to replace (8) by

$$\Pi_f p = \overline{p} + \frac{(2\xi - 1)\mu}{4\mathbf{K}_{f,\boldsymbol{\nu}}} b_f [\![\mathbf{v}^p \cdot \boldsymbol{\nu}]\!],\ \text{on } \Sigma,$$

where $\xi \geq 1/2$ is a quadrature parameter.

For example, the trapezoidal rule (8) is recovered when $\xi = 1/2$ which appears to be the most natural and simple choice, whereas the use of the mid-point rule gives $\xi = 3/4$. We give some numerical comparison of the models for various values of this parameter in Section 5.

Finally, the asymptotic model we study in this paper is (together with equations (1)-(4)):

$$\nabla_{\boldsymbol{\tau}} \cdot (b_f \mathbf{u}_{f,\boldsymbol{\tau}}) = b_f Q_f - [\![\mathbf{v}^p \cdot \boldsymbol{\nu}]\!] \text{ in } \Sigma, \tag{10}$$

$$\mathbf{u}_{f,\boldsymbol{\tau}} = -\frac{\mathbf{K}_{f,\boldsymbol{\tau}}}{\mu} \left(\nabla_{\boldsymbol{\tau}} \Pi_f p - \rho \, \mathbf{g} \cdot \boldsymbol{\tau}\right) \text{ in } \Sigma, \tag{11}$$

$$\overline{\mathbf{v}^p \cdot \boldsymbol{\nu}} = -\frac{\mathbf{K}_{f,\boldsymbol{\nu}}}{\mu} \left(\frac{[\![p]\!]}{b_f} - \rho \, \mathbf{g} \cdot \boldsymbol{\nu}\right) \text{ in } \Sigma, \tag{12}$$

$$\Pi_f p = \overline{p} + \frac{(2\xi - 1)\mu}{4\mathbf{K}_{f,\boldsymbol{\nu}}} b_f [\![\mathbf{v}^p \cdot \boldsymbol{\nu}]\!] \text{ in } \Sigma. \tag{13}$$

Formally, when $b_f \to 0$, we see from (10) and (12) that $[\![\mathbf{v}^p \cdot \boldsymbol{\nu}]\!]$ and $[\![p]\!]$ are enforced to tend to 0 on Σ. Furthermore, $b_f \mathbf{K}_{f,\boldsymbol{\tau}}$ and $\frac{\mathbf{K}_{f,\boldsymbol{\nu}}}{b_f}$ can be understood as equivalent tangential (resp. normal) permeabilities of the sharp fracture limit.

2.2.3. *Bibliographical remarks*

These models were already studied in [18] in the particular case where the fracture interface Σ is not immersed inside the domain $\widetilde{\Omega}$, but separates it into disjoint subdomains and for the quadrature parameter $\xi > 1/2$ (typically $\xi = 3/4$ or $\xi = 1$). In this reference, the most natural model (that is when $\xi = 1/2$) does not enter the analysis because of the mixed formulation considered. In particular, the mixed finite element approximation used there seems to yield numerical instabilities when $\xi \to 1/2$. The model with $\xi = 3/4$ is also numerically studied in [13] for an isotropic fracture permeability tensor $\mathbf{K}_f$.

In the case of fully immersed fracture, the asymptotic model is numerically experimented in [8] for $\xi = 3/4$. In [3–5], it is proposed (in the case $\xi = 1/2$) to replace the partial differential equation (10)-(11) on the fracture by a simpler algebraic model. More precisely, in these references, equations (1)-(4) and (12)-(13) are conserved whereas (10)-(11) are replaced by

$$[\![\mathbf{v}^p \cdot \boldsymbol{\nu}]\!] = -\frac{b_f \mathbf{K}_{f,\boldsymbol{\tau}}}{\mu} \left(\frac{1}{s}(\overline{p} - P) - \rho \, \mathbf{g} \cdot \boldsymbol{\tau}\right) + b_f Q_f \quad \text{on } \Sigma,$$

where P is a given reference pressure at $s = 0$. The coupling of these last models with solutal transport problems was also numerically experimented in [6].

3. Well-posedness of the asymptotic models

3.1. **Functional setting**

3.1.1. *Trace results for fractured domains*

We define $H^1_\Gamma(\Omega) = \{p \in H^1(\Omega), \quad p = 0 \text{ on } \Gamma\}$. Let us recall the trace theorems available for the fractured domain Ω (see for instance [15]). We concentrate here on the trace problem on the fracture Σ since the trace operator γ_Γ on Γ can be defined classically.

First of all, we define two linear and continuous trace operators γ^+ and γ^- from $H^1(\Omega)$ on $H^{\frac{1}{2}}(\Sigma)$, for instance by using the standard trace operators on the two domains Ω^+ and Ω^- and showing that the restriction to Σ to these traces does not depend on the way Ω^+ and Ω^- are constructed from the interface Σ.

We can also prove that the space $\mathcal{S}$ defined by

$$\mathcal{S} = \{u \in \mathcal{C}^\infty(\Omega) \cap \mathcal{C}^\infty(\bar{\Omega}^+) \cap \mathcal{C}^\infty(\bar{\Omega}^-), \, u \text{ is constant near the extremities of } \Sigma\}, \tag{14}$$

is dense in $H^1(\Omega)$.

Proposition 3.1. *The global trace operator γ_Σ on Σ defined by*

$$\gamma_\Sigma : p \in H^1(\Omega) \mapsto \gamma_\Sigma(p) = (\gamma^+(p), \gamma^-(p)) \in H^{\frac{1}{2}}(\Sigma) \times H^{\frac{1}{2}}(\Sigma),$$

is continuous from $H^1(\Omega)$ onto the space

$$\begin{aligned} T_\Sigma &= \left\{ (g^+, g^-) \in \left(H^{\frac{1}{2}}(\Sigma)\right)^2, \quad \int_0^{|\Sigma|} \frac{|g^+(s) - g^-(s)|^2}{s(|\Sigma| - s)}\, ds < +\infty \right\} \\ &= \left\{ (g^+, g^-) \in \left(H^{\frac{1}{2}}(\Sigma)\right)^2, \quad g^+ - g^- \in H^{\frac{1}{2}}_{00}(\Sigma) \right\}, \end{aligned}$$

endowed with the norm

$$\|(g^+, g^-)\|_{T_\Sigma} = \left(\|g^+\|^2_{H^{\frac{1}{2}}} + \|g^-\|^2_{H^{\frac{1}{2}}} + \int_0^{|\Sigma|} \frac{|g^+(s) - g^-(s)|^2}{s(|\Sigma| - s)}\, ds \right)^{\frac{1}{2}}.$$

Furthermore, there exists a continuous linear operator $R_\Sigma : T_\Sigma \to H^1_\Gamma(\Omega)$ which is a right inverse of the global trace operator, that is

$$\gamma_\Sigma \circ R_\Sigma = \mathrm{Id}_{T_\Sigma}.$$

Finally, $\mathcal{C}^\infty_c(\Omega)$ is dense in $\ker \gamma_\Sigma \cap H^1_\Gamma(\Omega)$.

One can now define the normal traces on Σ of any vector field in $\mathbf{v} \in H_{\mathrm{div}}(\Omega) \stackrel{\mathrm{def}}{=} \{\mathbf{u} \in (L^2(\Omega))^d, \quad \nabla \cdot \mathbf{u} \in L^2(\Omega)\}$ as follows.

Proposition 3.2. *The map $\mathbf{v} \cdot \mathbf{n}$ defined by*

$$g = (g^+, g^-) \in T_\Sigma \mapsto (\mathbf{v} \cdot \mathbf{n})(g) \stackrel{\mathrm{def}}{=} \int_\Omega \mathbf{v} \cdot \nabla R_\Sigma(g)\, dx + \int_\Omega (\nabla \cdot \mathbf{v}) R_\Sigma(g)\, dx,$$

is linear continuous and does not depend on the choice of the right inverse operator R_Σ. Furthermore, there exists two unique elements in $(H^{\frac{1}{2}}(\Sigma))'$ and $H^{-\frac{1}{2}}(\Sigma) = (H^{\frac{1}{2}}_{00}(\Sigma))'$ respectively denoted by $[\![\mathbf{v} \cdot \boldsymbol{\nu}]\!]$ and $\overline{\mathbf{v} \cdot \boldsymbol{\nu}}$ such that

$$\langle \mathbf{v} \cdot \mathbf{n}, g \rangle_{T_\Sigma', T_\Sigma} = -\left\langle [\![\mathbf{v} \cdot \boldsymbol{\nu}]\!], \frac{g^+ + g^-}{2} \right\rangle_{(H^{\frac{1}{2}})'(\Sigma), H^{\frac{1}{2}}(\Sigma)} - \langle \overline{\mathbf{v} \cdot \boldsymbol{\nu}}, (g^+ - g^-) \rangle_{H^{-\frac{1}{2}}(\Sigma), H^{\frac{1}{2}}_{00}(\Sigma)}.$$

When $\mathbf{v}$ is smooth enough (say $\mathbf{v} \in (H^1(\Omega))^d$), $[\![\mathbf{v} \cdot \boldsymbol{\nu}]\!]$ and $\overline{\mathbf{v} \cdot \boldsymbol{\nu}}$ are respectively equal to the jump and the mean-value of $\mathbf{v} \cdot \boldsymbol{\nu}$ across Σ.

Finally, we have for any $\phi \in H^1(\Omega)$ the following Stokes formula

$$\int_\Omega \mathbf{v} \cdot \nabla \phi\, dx + \int_\Omega (\nabla \cdot \mathbf{v}) \phi\, dx = \langle \mathbf{v} \cdot \mathbf{n}, \gamma_\Gamma \phi \rangle_{H^{-\frac{1}{2}}(\Gamma), H^{\frac{1}{2}}(\Gamma)} - \langle [\![\mathbf{v} \cdot \boldsymbol{\nu}]\!], \overline{\phi} \rangle_{(H^{\frac{1}{2}})'(\Sigma), H^{\frac{1}{2}}(\Sigma)} - \langle \overline{\mathbf{v} \cdot \boldsymbol{\nu}}, [\![\phi]\!] \rangle_{H^{-\frac{1}{2}}(\Sigma), H^{\frac{1}{2}}_{00}(\Sigma)}. \quad (15)$$

3.1.2. *Functional spaces*

From now on, we assume given the fracture aperture $s \mapsto b_f(s)$ such that

$$b_f \in \mathcal{C}^1(\Sigma), \quad \inf_\Sigma b_f > 0. \quad (16)$$

The gravity vector $\mathbf{g}$, the density ρ and the viscosity μ of the fluid as well as the quadrature parameter $\xi \in \left[\frac{1}{2}, +\infty\right[$ appearing in the model are fixed all along the following analysis.

We denote by $\|\cdot\|_{0,\Omega}$ the L^2-norm on Ω and $\|\cdot\|_{1,\Omega}$ the H^1-norm on Ω. Let $L^2(\Sigma)$ and $H^1(\Sigma)$ be the standard Lebesgue and Sobolev spaces on Σ endowed with their respective usual norms $\|\cdot\|_{0,\Sigma}$ and $\|\cdot\|_{1,\Sigma}$. For any pressure field $q \in H^1(\Omega)$ defined inside the porous matrix, let us associate the Darcy velocity $\mathbf{v}^q \in (L^2(\Omega))^2$ defined by

$$\mathbf{v}^q = -\frac{\mathbf{K}}{\mu}(\nabla q - \rho \mathbf{g}), \tag{17}$$

and, in the case where $\mathbf{v}^q \in H_{\rm div}(\Omega)$, we define the fracture pressure $\Pi_f q$ on Σ by

$$\Pi_f q = \overline{q} + \frac{(2\xi-1)\mu}{4\mathbf{K}_{f,\boldsymbol{\nu}}} b_f [\![\mathbf{v}^q \cdot \boldsymbol{\nu}]\!] \in (H^{\frac{1}{2}}(\Sigma))'. \tag{18}$$

Notice that the product $b_f[\![\mathbf{v}^q \cdot \boldsymbol{\nu}]\!]$ is well defined since b_f is supposed to be smooth (see (16)). We introduce the space

$$\mathcal{W} = \left\{ q \in H^1(\Omega) \text{ such that } \mathbf{v}^q \in H_{\rm div}(\Omega),\ (2\xi-1)[\![\mathbf{v}^q \cdot \boldsymbol{\nu}]\!] \in L^2(\Sigma), \Pi_f q \in H^1(\Sigma) \right\},$$

endowed with the norm

$$\|q\|_{\mathcal{W}} = \left(\|q\|_{1,\Omega}^2 + \|\Pi_f q\|_{1,\Sigma}^2 + (2\xi-1)\|[\![\mathbf{v}^q \cdot \boldsymbol{\nu}]\!]\|_{0,\Sigma}^2 \right)^{\frac{1}{2}}.$$

3.2. **Well-posedness of the problem**

We call *a solution of the asymptotic model*, any function $p \in \mathcal{W}$ that satisfies

$$\begin{aligned}
\nabla \cdot \mathbf{v}^p &= Q \text{ in } \Omega, && (19)\\
p &= p^D \text{ on } \Gamma_D, && (20)\\
\mathbf{v}^p \cdot \mathbf{n} &= 0 \text{ on } \Gamma_N, && (21)\\
-\nabla_{\boldsymbol{\tau}} \cdot \left(b_f \frac{\mathbf{K}_{f,\boldsymbol{\tau}}}{\mu} \left(\nabla_{\boldsymbol{\tau}} \Pi_f p - \rho\, \mathbf{g} \cdot \boldsymbol{\tau} \right) \right) &= b_f Q_f - [\![\mathbf{v}^p \cdot \boldsymbol{\nu}]\!] \text{ in } \Sigma, && (22)\\
-\frac{\mathbf{K}_{f,\boldsymbol{\tau}}}{\mu} \left(\nabla_{\boldsymbol{\tau}} \Pi_f p - \rho\, \mathbf{g} \cdot \boldsymbol{\tau} \right) &= 0 \text{ on } \partial\Sigma, && (23)\\
\overline{\mathbf{v}^p \cdot \boldsymbol{\nu}} &= -\frac{\mathbf{K}_{f,\boldsymbol{\nu}}}{\mu} \left(\frac{[\![p]\!]}{b_f} - \rho\, \mathbf{g} \cdot \boldsymbol{\nu} \right) \text{ on } \Sigma, && (24)
\end{aligned}$$

where $\mathbf{v}^p$ and $\Pi_f p$ are defined in (17)-(18) above.

Our first result is the following.

Theorem 3.3. *For any $\xi \geq \frac{1}{2}$, the problem* (19)-(24) *admits a unique solution $p \in \mathcal{W}$.*
Proof.

- **Existence:** This will be proved in the following section by passing to the limit in the finite volume scheme.

- **Uniqueness:** The problem being linear, it is enough to show that if $p \in \mathcal{W}$ is a solution to the homogeneous problem

$$\begin{aligned}
\widetilde{\mathbf{v}^p} &= -\frac{\mathbf{K}}{\mu}\nabla p, \text{ in } \Omega, && (25)\\
\nabla \cdot \widetilde{\mathbf{v}^p} &= 0 \text{ in } \Omega, && (26)\\
p &= 0, \text{ on } \Gamma_D, && (27)\\
\widetilde{\mathbf{v}^p} \cdot \mathbf{n} &= 0 \text{ on } \Gamma_N, && (28)\\
-\nabla_{\boldsymbol{\tau}} \cdot \left(b_f \frac{\mathbf{K}_{f,\boldsymbol{\tau}}}{\mu} \nabla_{\boldsymbol{\tau}} \Pi_f p \right) &= -[\![\widetilde{\mathbf{v}^p} \cdot \boldsymbol{\nu}]\!] \text{ on } \Sigma, && (29)\\
-\frac{\mathbf{K}_{f,\boldsymbol{\tau}}}{\mu} \nabla_{\boldsymbol{\tau}} \Pi_f p &= 0 \text{ on } \partial\Sigma, && (30)\\
\overline{\widetilde{\mathbf{v}^p} \cdot \boldsymbol{\nu}} &= -\frac{\mathbf{K}_{f,\boldsymbol{\nu}}}{\mu} \frac{[\![p]\!]}{b_f} \text{ on } \Sigma, && (31)
\end{aligned}$$

then we have $p = 0$.

To this end, we use p as a test function in (26), and using the Stokes formula (15), we get

$$\begin{aligned}
0 &= \int_\Omega p \, \nabla \cdot \widetilde{\mathbf{v}^p} \, dx \\
&= \int_\Omega \frac{\mathbf{K}}{\mu} |\nabla p|^2 \, dx - \langle [\![\widetilde{\mathbf{v}^p} \cdot \boldsymbol{\nu}]\!], \overline{p} \rangle_{(H^{\frac{1}{2}}(\Sigma))', H^{\frac{1}{2}}(\Sigma)} - \langle \overline{\widetilde{\mathbf{v}^p} \cdot \boldsymbol{\nu}}, [\![p]\!] \rangle_{H^{-\frac{1}{2}}(\Sigma), H^{\frac{1}{2}}_{00}(\Sigma)} \\
&= \int_\Omega \frac{\mathbf{K}}{\mu} |\nabla p|^2 \, dx - \langle [\![\widetilde{\mathbf{v}^p} \cdot \boldsymbol{\nu}]\!], \overline{p} \rangle_{(H^{\frac{1}{2}}(\Sigma))', H^{\frac{1}{2}}(\Sigma)} + \int_\Sigma \frac{\mathbf{K}_{f,\boldsymbol{\nu}}}{\mu} \left| \frac{[\![p]\!]}{b_f(s)} \right|^2 b_f(s) \, ds.
\end{aligned}$$

Since $p \in \mathcal{W}$, we can use $\Pi_f p \in H^1_{b_f}(\Sigma)$ as a test function in (29) with the boundary condition (30). We get

$$0 = \int_\Sigma \frac{\mathbf{K}_{f,\boldsymbol{\tau}}}{\mu} |\nabla_{\boldsymbol{\tau}} \Pi_f p|^2 b_f \, ds + \langle [\![\widetilde{\mathbf{v}^p} \cdot \boldsymbol{\nu}]\!], \Pi_f p \rangle_{(H^{\frac{1}{2}}(\Sigma))', H^{\frac{1}{2}}(\Sigma)}.$$

Adding the previous two equalities and using the definition (18) of $\Pi_f p$, it follows

$$\int_\Omega \frac{\mathbf{K}}{\mu} |\nabla p|^2 \, dx + \int_\Sigma \frac{\mathbf{K}_{f,\boldsymbol{\tau}}}{\mu} |\nabla_{\boldsymbol{\tau}} \Pi_f p|^2 b_f \, ds + \int_\Sigma \frac{\mathbf{K}_{f,\boldsymbol{\nu}}}{\mu} \left| \frac{[\![p]\!]}{b_f} \right|^2 b_f \, ds + \frac{(2\xi - 1)\mu}{4\mathbf{K}_{f,\boldsymbol{\nu}}} \int_\Sigma [\![\widetilde{\mathbf{v}^p} \cdot \boldsymbol{\nu}]\!]^2 b_f \, ds = 0.$$

We conclude, since $\xi \geq \frac{1}{2}$, and using (27), that the unique solution $p \in \mathcal{W}$ of (26)-(32) is $p = 0$, which proves that problem (19)-(24) has at most one solution in $\mathcal{W}$.

□

Remark 3.4. Existence and uniqueness of a solution to problem (19)-(24) can also be proved in the case $\xi > \frac{1}{2}$ by using a mixed formulation (see [18] in the case of the non-immersed fracture, that is when $\tilde{\Omega} \setminus \Sigma$ is not connected). For $\xi = \frac{1}{2}$ the coercivity of the mixed formulation is no more satisfied. Nevertheless, we can recover the result (for instance when $p^D = 0$) by using the Lax-Milgram theorem for the following variational problem

$$\text{Find } p \in \mathcal{W}_0 \text{ such that } a(p, q) = L(q) \text{ for all } q \in \mathcal{W}_0,$$

where $\mathcal{W}_0 = \mathcal{W} \cap {\gamma_{0,D}}^{-1}(\{0\})$, and a is the bilinear form on $\mathcal{W}_0$ defined by

$$a(p,q) = \frac{1}{\mu}\int_\Omega \mathbf{K}\nabla p \cdot \nabla q \, dx + \int_\Sigma \frac{\mathbf{K}_{f,\boldsymbol{\tau}}}{\mu}\nabla_{\boldsymbol{\tau}}\Pi_f p \nabla_{\boldsymbol{\tau}}\Pi_f q \, b_f \, ds + \int_\Sigma \frac{\mathbf{K}_{f,\boldsymbol{\nu}}}{\mu}\frac{[\![p]\!]}{b_f}\frac{[\![q]\!]}{b_f} \, b_f \, ds$$

and L is the linear form

$$L(q) = \int_\Omega Qq \, dx + \int_\Sigma b_f Q_f \Pi_f q \, ds + \frac{1}{\mu}\int_\Omega \rho \mathbf{K}\mathbf{g}\cdot\nabla q \, dx + \int_\Sigma \frac{\mathbf{K}_{f,\boldsymbol{\tau}}}{\mu}\rho\mathbf{g}\cdot\boldsymbol{\tau}\nabla_{\boldsymbol{\tau}} q \, b_f \, ds + \int_\Sigma \frac{\mathbf{K}_{f,\boldsymbol{\tau}}}{\mu}\rho\mathbf{g}\cdot\boldsymbol{\nu}[\![q]\!] \, ds.$$

Indeed, since $\xi = 1/2$, $\mathcal{W}_0$ is an Hilbert space and the bilinear form a is continuous and coercive on $\mathcal{W}_0$ and the linear form L is continuous on $\mathcal{W}_0$. We can check that the solution p to this variational formulation actually solves the problem under study (see the end of the proof of Theorem 4.13)

4. Finite volume scheme for the asymptotic models

We restrict our attention here to a constant isotropic permeability tensor $\mathbf{K}$ in the porous matrix (so that we will abusively consider $\mathbf{K}$ as a positive real number) and to a constant diagonal (but not necessarily isotropic) permeability $\mathbf{K}_f$ tensor in the frame $(\boldsymbol{\tau}, \boldsymbol{\nu})$ associated to the fracture.

From now on, $p^D \in H^{\frac{1}{2}}(\Gamma_D)$ is a given boundary data for the pressure.

4.1. **Notations and assumptions for the polygonal mesh**

Let us define the notations we will use to describe and analyze our finite volume scheme. Most of the notations are inspired from [12], which is our reference for a general description and analysis of finite volume schemes for usual elliptic equations.

A mesh of the fractured domain $\Omega \cup \Sigma$ is denoted by $\mathcal{T} = (\mathfrak{M}, \mathfrak{S})$ where $\mathfrak{M}$ (resp. $\mathfrak{S}$) is a family of disjoint 2-dimensional control volumes $\kappa \subset \Omega$ (resp. 1-dimensional control volumes $\sigma \subset \Sigma$).

- The control volumes $\kappa \in \mathfrak{M}$ are open convex polygons such that $\overline{\Omega} = \cup_{\kappa\in\mathfrak{M}}\overline{\kappa}$. For any $(\kappa, \mathcal{L}) \in \mathfrak{M}^2$ with $\kappa \neq \mathcal{L}$, either $\overline{\kappa} \cap \overline{\mathcal{L}} = \emptyset$, a vertex, or $\overline{\kappa} \cap \overline{\mathcal{L}} = \overline{\sigma}$ for some edge $\sigma \equiv \kappa|\mathcal{L}$.

  Let $\mathcal{E}_{int}$ denote the set of interior edges $\sigma = \kappa|\mathcal{L} \subset \Omega$ and $\mathcal{E}_{ext}^D$, $\mathcal{E}_{ext}^N$ the sets of edges lying on the boundary Γ with $\sigma \subset \Gamma_D$ or $\sigma \subset \Gamma_N$ respectively. The set $\mathcal{E}$ of all the edges can then be decomposed in $\mathcal{E} = \mathcal{E}_{int} \cup \mathcal{E}_{ext}^D \cup \mathcal{E}_{ext}^N \cup \mathfrak{S}$.

  For each $\kappa \in \mathfrak{M}$, a discretization point $x_\kappa \in \kappa$ is chosen such that the segment $[x_\kappa, x_\mathcal{L}]$ is orthogonal at the point x_σ to each edge $\sigma = \kappa|\mathcal{L}$. Let $d_{\kappa,\sigma} > 0$ be the distance from x_κ to σ, and $d_{\kappa,\mathcal{L}} = d_{\kappa,\sigma} + d_{\mathcal{L},\sigma}$ the distance between x_κ and $x_\mathcal{L}$. The set of edges of κ is denoted by $\mathcal{E}_\kappa$. For each $\sigma \in \mathcal{E}_\kappa$, $\mathbf{n}_{\kappa,\sigma}$ is the outward unit normal of σ at κ.
- We assume that the meshes $\mathfrak{M}$ and $\mathfrak{S}$ are compatible, that is for any control volume $\sigma \in \mathfrak{S}$ there exists $(\kappa_\sigma^+, \kappa_\sigma^-) \in \mathfrak{M}^2$ such that $\sigma = \kappa_\sigma^+|\kappa_\sigma^-$ with $\kappa_\sigma^+ \subset \Omega^+$ and $\kappa_\sigma^- \subset \Omega^-$.

  We denote by $\mathfrak{V}$ the set of the vertices e of the mesh $\mathfrak{S}$ and by $\mathfrak{V}_{int}$ the set of such vertices which are not on the boundary $\partial\Sigma$ (see Figure 2), so that we have $\mathfrak{V} = \mathfrak{V}_{int} \cup \{\partial\Sigma^+, \partial\Sigma^-\}$. For each $\sigma \in \mathfrak{S}$, let $\mathcal{V}_\sigma$ be the set of vertices in $\mathfrak{V}$ belonging to $\partial\sigma$.

  To each point $e = \sigma|\sigma' \in \mathfrak{V}_{int}$ we associate the segment $S_e = [x_\sigma, x_{\sigma'}]$ and the unit vector $\boldsymbol{\tau}_{\sigma,\sigma'}$ pointing from x_σ towards $x_{\sigma'}$. For $e \in \{\partial\Sigma^-, \partial\Sigma^+\}$ we note $S_e = [x_\sigma, e]$ where $\sigma \in \mathfrak{S}$ is the unique element of $\mathfrak{S}$ such that $e \in \partial\sigma$. We note $\mathfrak{I} = (S_e)_{e\in\mathfrak{V}}$ the set of such segments.

For each $\kappa \in \mathfrak{M}$ or $\sigma \in \mathfrak{S}$, $m(\kappa)$ and $m(\sigma)$ denote the 2D-measure of κ, resp. the 1D-measure of σ. The mesh size is defined by : $\text{size}(\mathcal{T}) = \sup\{\text{diam}(\kappa),\ \kappa \in \mathfrak{M}\}$.

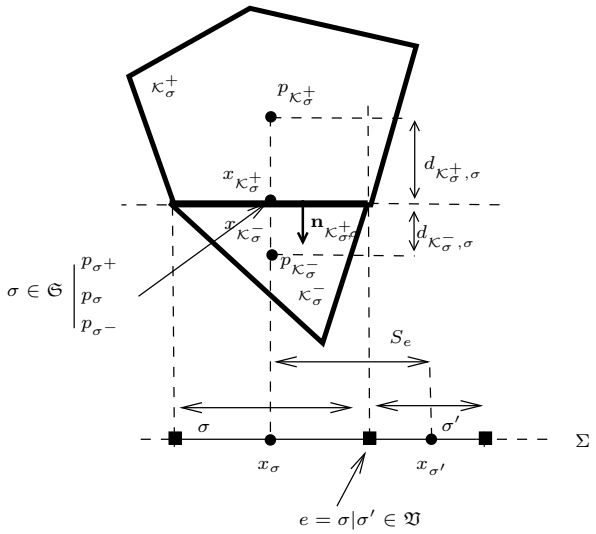

FIGURE 2. Geometry of the meshes along Σ

Finally, let $r_\mathcal{K} > 0$ be the larger radius of an open ball centered in $x_\mathcal{K}$ and contained in κ. The regularity of the mesh is then measured by the quantity

$$\mathrm{reg}(\mathcal{T}) = \max_{\kappa\in\mathfrak{M}} \frac{\mathrm{diam}(\kappa)}{r_\mathcal{K}},$$

that we will require to be bounded when the size of the mesh tends to 0 in our convergence results. The dependence of any quantity with respect to $\mathrm{reg}(\mathcal{T})$ is implicitly assumed to be non-increasing.

4.2. **The discrete spaces**

4.2.1. *The discrete unknowns*

- Matrix pressure field and its traces:
  We associate to the mesh $\mathcal{T}$ a set of discrete unknowns $p^\mathcal{T}$ composed as follows

$$p^\mathcal{T} = (p^\mathfrak{M}, \gamma_{0,N}p^\mathcal{T}, \gamma^+p^\mathcal{T}, \gamma^-p^\mathcal{T}) \in E(\mathcal{T}) \stackrel{\text{def}}{=} \mathbb{R}^\mathfrak{M} \times \mathbb{R}^{\mathcal{E}_{ext}^N} \times \mathbb{R}^\mathfrak{S} \times \mathbb{R}^\mathfrak{S}.$$

  The unknown vector $p^\mathfrak{M} = (p_\mathcal{K})_{\mathcal{K}\in\mathfrak{M}} \in \mathbb{R}^\mathfrak{M}$ contains the cell-centered unknowns on the mesh $\mathfrak{M}$, the vector $\gamma_{0,N}p^\mathcal{T} = (p_\sigma)_{\sigma\in\mathcal{E}_{ext}^N}$ represents the boundary values of the pressure on the part of the boundary where Neumann boundary conditions will be imposed. Since we are going to consider possible jumps of the pressure across the fracture Σ, we need to consider two different discrete traces of the pressure on Σ denoted by $\gamma^+p^\mathcal{T} \stackrel{\text{def}}{=} (p_{\sigma^+})_{\sigma\in\mathfrak{S}} \in \mathbb{R}^\mathfrak{S}$ and $\gamma^-p^\mathcal{T} \stackrel{\text{def}}{=} (p_{\sigma^-})_{\sigma\in\mathfrak{S}} \in \mathbb{R}^\mathfrak{S}$. The jumps and the mean-value across Σ of $p^\mathcal{T}$ is defined by $[\![p^\mathcal{T}]\!] = \gamma^+p^\mathcal{T} - \gamma^-p^\mathcal{T}$ and $\overline{p^\mathcal{T}} = (\gamma^+p^\mathcal{T} + \gamma^-p^\mathcal{T})/2$. We can finally define, the boundary value on Γ_D of any given $p^\mathfrak{M} \in \mathbb{R}^\mathcal{T}$ by $\gamma_{0,D}p^\mathfrak{M} = (p_{\mathcal{K}_\sigma})_{\sigma\in\mathcal{E}_{ext}^D} \in \mathbb{R}^{\mathcal{E}_{ext}^D}$, where κ_σ is the unique control volume in $\mathfrak{M}$ such that $\sigma \subset \partial\kappa_\sigma$.

  As usual, in order to state our convergence results, discrete functions are identified as piecewise constant functions as follows

$$p^\mathfrak{M} = \sum_{\kappa\in\mathfrak{M}} \mathbb{1}_\mathcal{K} p_\mathcal{K}, \quad \gamma^+p^\mathcal{T} = \sum_{\sigma\in\mathfrak{S}} \mathbb{1}_\sigma p_{\sigma^+}, \quad \gamma^-p^\mathcal{T} = \sum_{\sigma\in\mathfrak{S}} \mathbb{1}_\sigma p_{\sigma^-},$$

$$\gamma_{0,D} p^{\mathfrak{M}} = \sum_{\sigma \in \mathcal{E}_{ext}^D} \mathbb{1}_\sigma p_{\mathcal{K}_\sigma}, \quad \gamma_{0,N} p^{\mathcal{T}} = \sum_{\sigma \in \mathcal{E}_{ext}^N} \mathbb{1}_\sigma p_\sigma.$$

- Fracture pressure:
  We associate to the mesh $\mathfrak{S}$ on Σ, a fracture pressure unknown

$$p^{\mathfrak{S}} = ((p_\sigma)_{\sigma \in \mathfrak{S}}, p_{\partial\Sigma^-}, p_{\partial\Sigma^+}) \in E(\mathfrak{S}) \stackrel{\text{def}}{=} \mathbb{R}^{\mathfrak{S}} \times \mathbb{R} \times \mathbb{R},$$

  where p_σ is a value at the center x_σ of the edge σ and $p_{\partial\Sigma^-}$, $p_{\partial\Sigma^+}$ the boundary values at the two extremities $\partial\Sigma^-$ and $\partial\Sigma^+$ of Σ. We associate to $p^{\mathfrak{S}}$ a piecewise constant function on Σ still denoted by $p^{\mathfrak{S}}$ and defined $p^{\mathfrak{S}} \stackrel{\text{def}}{=} \sum_{\sigma \in \mathfrak{S}} \mathbb{1}_\sigma p_\sigma$. Fig. 2 sums up the different unknowns introduced near the fracture.

4.2.2. *Discrete gradient*

Let us define the diamond cells $\mathcal{D}_\sigma$ for $\sigma \in \mathcal{E}_{int} \cup \mathcal{E}_{ext}$ and $\mathcal{D}_{\sigma^+}, \mathcal{D}_{\sigma^-}$ for $\sigma \in \mathfrak{S}$ as shown in Figure 3. For $\sigma = \kappa|\mathcal{L} \in \mathcal{E}_{int}$, $\mathcal{D}_\sigma$ is the quadrangle whose diagonals are σ and $[x_\kappa, x_\mathcal{L}]$. The set of such diamond cells is called $\mathfrak{D}_{int}$. For $\sigma = \mathcal{E}_{ext} \cap \mathcal{E}_\kappa$, $\mathcal{D}_\sigma$ is the triangle defined by the point x_κ and the edge σ. The set of such diamond cells is called $\mathfrak{D}_{ext}$. Finally, for $\sigma \in \mathfrak{S}$, $\mathcal{D}_{\sigma^+}$ and $\mathcal{D}_{\sigma^-}$ are the two triangles defined by the edge σ and by the points $x_{\mathcal{K}_\sigma^+}$ and $x_{\mathcal{K}_\sigma^-}$ respectively. We note $\mathfrak{D}_{\Sigma^+} = \{\mathcal{D}_{\sigma^+}, \sigma \in \mathfrak{S}\}$, $\mathfrak{D}_{\Sigma^-} = \{\mathcal{D}_{\sigma^-}, \sigma \in \mathfrak{S}\}$ and $\mathfrak{D} = \mathfrak{D}_{int} \cup \mathfrak{D}_{ext} \cup \mathfrak{D}_{\Sigma^+} \cup \mathfrak{D}_{\Sigma^-}$.

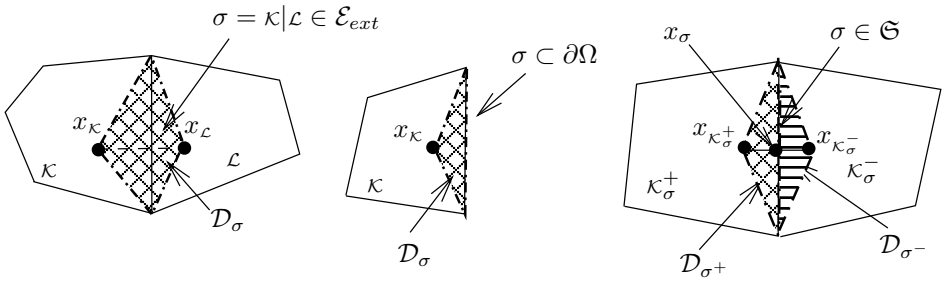

FIGURE 3. The diamond cells

Definition 4.1 (Discrete gradient on $\mathfrak{M}$)**.** For any $p^{\mathcal{T}} \in E(\mathcal{T})$, we define the vector-valued function $\nabla^{\mathfrak{M},p^D} p^{\mathcal{T}}$ by

$$\begin{aligned}\nabla^{\mathfrak{M},p^D} p^{\mathcal{T}} \stackrel{\text{def}}{=} 2\Bigg(&\sum_{\substack{\mathcal{D}_\sigma \in \mathfrak{D}_{int} \\ \sigma = \mathcal{K}|\mathcal{L}}} \mathbb{1}_{\mathcal{D}_\sigma} \frac{p_\mathcal{L} - p_\mathcal{K}}{d_{\mathcal{K},\mathcal{L}}} \mathbf{n}_{\mathcal{K}|\mathcal{L}} + \sum_{\substack{\mathcal{D}_\sigma \in \mathfrak{D}_{ext} \\ \sigma \subset \Gamma_D}} \mathbb{1}_{\mathcal{D}_\sigma} \frac{p_\sigma^D - p_{\mathcal{K}_\sigma}}{d_{\mathcal{K},\sigma}} \mathbf{n}_{\mathcal{K}_\sigma} + \sum_{\substack{\mathcal{D}_\sigma \in \mathfrak{D}_{ext} \\ \sigma \subset \Gamma_N}} \mathbb{1}_{\mathcal{D}_\sigma} \frac{p_\sigma - p_{\mathcal{K}_\sigma}}{d_{\mathcal{K},\sigma}} \mathbf{n}_{\mathcal{K},\sigma} \\ &+ \sum_{\mathcal{D}_{\sigma^+} \in \mathfrak{D}_{\Sigma^+}} \mathbb{1}_{\mathcal{D}_{\sigma^+}} \frac{p_{\sigma^+} - p_{\mathcal{K}_\sigma^+}}{d_{\mathcal{K}_\sigma^+,\sigma}} \mathbf{n}_{\mathcal{K}_\sigma^+} + \sum_{\mathcal{D}_{\sigma^-} \in \mathfrak{D}_{\Sigma^-}} \mathbb{1}_{\mathcal{D}_{\sigma^-}} \frac{p_{\sigma^-} - p_{\mathcal{K}_\sigma^-}}{d_{\mathcal{K}_\sigma^-,\sigma}} \mathbf{n}_{\mathcal{K}_\sigma^-} \Bigg),\end{aligned} \tag{32}$$

where $p_\sigma^D = \frac{1}{m(\sigma)} \int_\sigma p^D(s)\, ds$.

Definition 4.2 (Projection of the gravity term on the mesh)**.** We denote by $\Pi^{\mathfrak{D}}\mathbf{g}$ the piecewise constant vector-valued function defined by

$$\Pi^{\mathfrak{D}}\mathbf{g} = 2 \sum_{\mathcal{D}_\sigma \in \mathfrak{D}} \mathbb{1}_{\mathcal{D}_\sigma} (\mathbf{g} \cdot \mathbf{n}_\sigma) \mathbf{n}_\sigma.$$

The definition of such a discrete gradient was first proposed in [11] in order to study some links between homogenisation and numerical schemes. Notice that the coefficient 2 in front of the formula (32) is in fact the dimension $d = 2$ of the problem we are studying. Its presence is due to the fact that only the part of the

gradient along the normal $\mathbf{n}_\sigma$ is approximated on each diamond cell. As we will see in the proof of Lemma 4.10, this coefficient 2 actually appears to be necessary to reach the weak convergence of the discrete gradient toward the continuous one.

Definition 4.3 (Fluxes accross Σ)**.** For any $p^{\mathcal{T}} \in E(\mathcal{T})$, we introduce the two mass fluxes across any edge σ in $\mathfrak{S}$ by

$$\mathbf{v}_{\sigma^+}^{p^{\mathcal{T}}} \cdot \mathbf{n}^+ \stackrel{\text{def}}{=} -\frac{\mathbf{K}}{\mu}\left(\frac{p_{\sigma^+} - p_{\mathcal{K}_\sigma^+}}{d_{\mathcal{K}_\sigma^+,\sigma}} - \rho\mathbf{g}\cdot\mathbf{n}^+\right), \quad \mathbf{v}_{\sigma^-}^{p^{\mathcal{T}}} \cdot \mathbf{n}^- \stackrel{\text{def}}{=} -\frac{\mathbf{K}}{\mu}\left(\frac{p_{\sigma^-} - p_{\mathcal{K}_\sigma^-}}{d_{\mathcal{K}_\sigma^-,\sigma}} - \rho\mathbf{g}\cdot\mathbf{n}^-\right).$$

Finally, the jump and the mean-value of these fluxes are defined by

$$\begin{cases} [\![\mathbf{v}_\sigma^{p^{\mathcal{T}}} \cdot \boldsymbol{\nu}]\!] \stackrel{\text{def}}{=} -(\mathbf{v}_{\sigma^+}^{p^{\mathcal{T}}} \cdot \mathbf{n}^+ + \mathbf{v}_{\sigma^-}^{p^{\mathcal{T}}} \cdot \mathbf{n}^-), \\ \overline{\mathbf{v}_\sigma^{p^{\mathcal{T}}} \cdot \boldsymbol{\nu}} \stackrel{\text{def}}{=} -\dfrac{\mathbf{v}_{\sigma^+}^{p^{\mathcal{T}}} \cdot \mathbf{n}^+ - \mathbf{v}_{\sigma^-}^{p^{\mathcal{T}}} \cdot \mathbf{n}^-}{2}. \end{cases} \tag{33}$$

Definition 4.4 (Discrete fracture pressure)**.** For any matrix pressure field $p^{\mathcal{T}} \in E(\mathcal{T})$, following (18), we define the discrete fracture pressure $\Pi^{\mathfrak{S}} p^{\mathcal{T}} \in E(\mathfrak{S})$ associated to $p^{\mathcal{T}}$ by

$$\Pi^{\mathfrak{S}} p^{\mathcal{T}} = \frac{1}{2}\left(\gamma^+ p^{\mathcal{T}} + \gamma^- p^{\mathcal{T}}\right) + \frac{(2\xi-1)\mu}{4\mathbf{K}_{f,\boldsymbol{\nu}}} b_{f,\sigma} [\![\mathbf{v}^{p^{\mathcal{T}}} \cdot \boldsymbol{\nu}]\!],$$

where $b_{f,\sigma}$ is the mean value of b_f on σ.

Definition 4.5 (Discrete gradient on $\mathfrak{S}$)**.** For any fracture pressure field $p^{\mathfrak{S}} \in E(\mathfrak{S})$, we define the real-valued function $\nabla^{\mathfrak{S}} p^{\mathfrak{S}} \in L^2(\Sigma)$ by

$$\nabla^{\mathfrak{S}} p^{\mathfrak{S}} = \sum_{\substack{e \in \mathfrak{V}_{int} \\ e=\sigma|\sigma'}} \mathbb{1}_{S_e} \frac{p_{\sigma'} - p_\sigma}{m(S_e)} (\boldsymbol{\tau}_{\sigma,\sigma'} \cdot \boldsymbol{\tau}) + \mathbb{1}_{S_{\partial\Sigma^+}} \frac{p_{\partial\Sigma^+} - p_{\sigma^+}}{m(S_{\partial\Sigma^+})} - \mathbb{1}_{S_{\partial\Sigma^-}} \frac{p_{\partial\Sigma^-} - p_{\sigma^-}}{m(S_{\partial\Sigma^-})}.$$

4.2.3. *The discrete norms*

We define on $E(\mathcal{T})$ the discrete $H^1(\Omega)$ norm

$$\|p^{\mathcal{T}}\|_{1,\mathcal{T}} = \left(\|p^{\mathfrak{M}}\|_{0,\Omega}^2 + \|\nabla^{\mathfrak{M},p^D} p^{\mathcal{T}}\|_{0,\Omega}^2\right)^{\frac{1}{2}},$$

and on $E(\mathfrak{S})$, the discrete $H^1(\Sigma)$ norm

$$\|p^{\mathfrak{S}}\|_{1,\mathfrak{S}} = \left(\|p^{\mathfrak{S}}\|_{0,\Sigma}^2 + \|\nabla^{\mathfrak{S}} p^{\mathfrak{S}}\|_{0,\Sigma}^2\right)^{\frac{1}{2}}.$$

Finally, we define on $E(\mathcal{T})$ the discrete W norm by

$$\|p^{\mathcal{T}}\|_{W^{\mathcal{T},p^D}} = \left(\|p^{\mathcal{T}}\|_{1,\mathcal{T}}^2 + \|\Pi^{\mathfrak{S}} p^{\mathcal{T}}\|_{1,\mathfrak{S}}^2 + (2\xi-1)\|[\![\mathbf{v}^{p^{\mathcal{T}}} \cdot \boldsymbol{\nu}]\!]\|_{0,\Sigma}^2\right)^{\frac{1}{2}}. \tag{34}$$

Lemma 4.6 (Discrete trace inequality)**.** *There exists $C > 0$ depending on* $\mathrm{reg}(\mathcal{T})$ *such that for all $p^{\mathcal{T}} \in E(\mathcal{T})$, we have*

$$\|\gamma_0 p^{\mathfrak{M}}\|_{0,\Gamma} + \|\gamma^+ p^{\mathcal{T}}\|_{0,\Sigma} + \|\gamma^- p^{\mathcal{T}}\|_{0,\Sigma} \le C\|p^{\mathcal{T}}\|_{1,\mathcal{T}}.$$

Lemma 4.7 (Discrete Poincaré Lemma)**.** *There exists $C = C(\Omega)$ such that for all $p^{\mathcal{T}} \in E(\mathcal{T})$, we have*

$$\|p^{\mathfrak{M}}\|_{0,\Omega} \leq C \left(\|\nabla^{\mathfrak{M},p^D} p^{\mathcal{T}}\|_{0,\Omega} + \|p^D\|_{\frac{1}{2},\Gamma_D} \right).$$

The proofs of Lemmas 4.6 and 4.7 are direct adaptations of the one for classical analogous results given in [12] for instance.

4.3. **The cell-centered numerical scheme**

4.3.1. *Description of the scheme*

- **Flow in the porous matrix Ω.** Integrating equation (19) over all control volumes $\kappa \in \mathfrak{M}$, the classical cell-centered FV method reads

$$\sum_{\sigma \in \mathcal{E}_\kappa} F_{\kappa,\sigma} = m(\kappa) Q_\kappa, \qquad \forall \kappa \in \mathfrak{M}, \tag{35}$$

where Q_κ is the mean value of Q on κ, and $F_{\kappa,\sigma}$ is the numerical flux approaching $\int_\sigma \mathbf{v}^p \cdot \mathbf{n}_\kappa \, ds$. This numerical flux is defined by

$$F_{\kappa,\sigma} \overset{\text{def}}{=} -m(\sigma) \frac{\mathbf{K}}{\mu} \left(\frac{p_{\kappa,\sigma} - p_\kappa}{d_{\kappa,\sigma}} - \rho \mathbf{g} \cdot \mathbf{n}_\kappa \right),$$

where $p_{\kappa,\sigma}$ is an approximate value of the pressure on the side of σ touching the control volume κ. Let us see how to determine $p_{\kappa,\sigma}$.

  - For $\sigma = \kappa|\mathcal{L} \in \mathcal{E}_{int}$, the pressure is continuous across σ, that is $p_{\kappa,\sigma} = p_{\mathcal{L},\sigma}$, and we have conservativity of the fluxes, that is $F_{\kappa,\sigma} = -F_{\kappa,\sigma}$. It follows in that case that $p_{\kappa,\sigma} = p_{\mathcal{L},\sigma}$ can be eliminated and we get

$$F_{\kappa,\mathcal{L}} \overset{\text{def}}{=} F_{\kappa,\sigma} = -F_{\mathcal{L},\sigma} = -m(\sigma) \frac{\mathbf{K}}{\mu} \left(\frac{p_\mathcal{L} - p_\kappa}{d_{\kappa,\mathcal{L}}} - \rho \mathbf{g} \cdot \mathbf{n}_{\kappa,\mathcal{L}} \right). \tag{36}$$

  - For $\sigma \in \mathcal{E}_{ext}^N$, then $p_{\kappa,\sigma}$ is the corresponding value p_σ of $\gamma_{0,N} p^{\mathcal{T}}$ and the Neumann boundary condition reads $F_{\kappa_\sigma,\sigma} = 0$, which determines in fact p_σ. We do not really need its value since the important point is that the numerical flux is zero.
  - For $\sigma \in \mathcal{E}_{ext}^D$, then $p_{\kappa,\sigma}$ is given by the mean value p_σ^D of the Dirichlet data p^D on σ, then

$$F_{\kappa_\sigma,\sigma} = -m(\sigma) \frac{\mathbf{K}}{\mu} \left(\frac{p_\sigma^D - p_{\kappa_\sigma}}{d_{\kappa,\sigma}} - \rho \mathbf{g} \cdot \mathbf{n}_\kappa \right). \tag{37}$$

  - For $\sigma \in \mathfrak{S}$, then the pressure is not continuous across σ, and is defined by $\gamma^{\pm} p^{\mathcal{T}}$ on each side of σ. More precisely, we have

$$F_{\kappa_\sigma^+,\sigma} = -m(\sigma) \frac{\mathbf{K}}{\mu} \left(\frac{p_{\sigma^+} - p_{\kappa_\sigma^+}}{d_{\kappa_\sigma^+,\sigma}} - \rho \mathbf{g} \cdot \mathbf{n}^+ \right),$$

and

$$F_{\kappa_\sigma^-,\sigma} = -m(\sigma) \frac{\mathbf{K}}{\mu} \left(\frac{p_{\sigma^-} - p_{\kappa_\sigma^-}}{d_{\kappa_\sigma^-,\sigma}} - \rho \mathbf{g} \cdot \mathbf{n}^- \right).$$

In this case, we do not have conservativity of the fluxes and the values of p_{σ^+} and p_{σ^-} will be determined through the coupling with the discretization of the 1D elliptic equation (22) on Σ.

Note that, following Definition 4.3, we have

$$F_{\mathcal{K}_\sigma^+,\sigma} = m(\sigma)\mathbf{v}_{\sigma^+}^{p^\mathcal{T}} \cdot \mathbf{n}^+, \quad F_{\mathcal{K}_\sigma^-,\sigma} = m(\sigma)\mathbf{v}_{\sigma^-}^{p^\mathcal{T}} \cdot \mathbf{n}^-. \tag{38}$$

- **The discrete fracture pressure.** The discrete fracture pressure is now defined by $p^\mathfrak{S} \overset{\text{def}}{=} \Pi^\mathfrak{S} p^\mathcal{T}$. Following Definition 4.4, this reads

$$p_\sigma = \frac{1}{2}(p_{\sigma^+} + p_{\sigma^-}) + \frac{(2\xi-1)\mu}{4\mathbf{K}_{f,\boldsymbol{\nu}}} b_{f,\sigma}[\![\mathbf{v}_\sigma^{p^\mathcal{T}} \cdot \boldsymbol{\nu}]\!], \quad \forall \sigma \in \mathfrak{S}. \tag{39}$$

- **Flow along the fracture Σ.** The 1D finite volume discretization of problem (22)-(23) reads

$$\sum_{e\in\mathcal{V}_\sigma} G_{\sigma,e} = m(\sigma) b_{f,\sigma} Q_{f,\sigma} - m(\sigma)[\![\mathbf{v}_\sigma^{p^\mathcal{T}} \cdot \boldsymbol{\nu}]\!], \quad \forall \sigma \in \mathfrak{S}, \tag{40}$$

where $Q_{f,\sigma} = \frac{1}{b_{f,\sigma} m(\sigma)} \int_\sigma Q_f(s) b_f(s)\, ds$. The numerical flux $G_{\sigma,e}$ aims to approach $-\frac{\mathbf{K}_{f,\boldsymbol{\tau}}}{\mu} b_f(\nabla_{\boldsymbol{\tau}} \Pi_f p - \rho \mathbf{g}\cdot\boldsymbol{\tau})$ at the vertex e. This flux is defined by

$$G_{\sigma,e} = -\frac{\mathbf{K}_{f,\boldsymbol{\tau}}}{\mu} b_{f,e} \left(\frac{p_{\sigma,e} - p_\sigma}{d_{\sigma,\sigma'}} - \rho \mathbf{g}\cdot\boldsymbol{\tau}_{\sigma,\sigma'} \right),$$

where $b_{f,e}$ is the mean value of b_f on the segment $[x_\sigma, x_{\sigma'}]$ and $p_{\sigma,e}$ is an approximate value of the fracture pressure at the vertex e.

  - For $e = \sigma|\sigma \in \mathfrak{V}_{int}$, we use the conservativity of the fluxes $G_{\sigma,e} = -G_{\sigma',e}$ and the continuity of the pressure $p_{\sigma,e} = p_{\sigma',e}$, so that the fluxes finally reads

$$G_{\sigma,\sigma'} \overset{\text{def}}{=} G_{\sigma,e} = -G_{\sigma',e} = -\frac{\mathbf{K}_{f,\boldsymbol{\tau}}}{\mu} b_{f,e} \left(\frac{p_{\sigma'} - p_\sigma}{d_{\sigma,e}} - \rho \mathbf{g}\cdot\boldsymbol{\tau}_{\sigma,\sigma'} \right). \tag{41}$$

  - For $e \in \partial\Sigma = \{\partial\Sigma^+, \partial\Sigma^-\}$, the value $p_{\sigma,e}$ is given by $p_{\partial\Sigma^-}$ or $p_{\partial\Sigma^+}$ and the Neumann boundary condition (23) implies that $G_{\sigma,e} = 0$. This uniquely defines the two boundary values $p_{\partial\Sigma^-}$ and $p_{\partial\Sigma^+}$.

- **Transmission conditions on Σ.** The discretization of equation (24) for all $\sigma = \kappa_\sigma^+|\kappa_\sigma^- \in \mathfrak{S}$ gives :

$$\overline{\mathbf{v}_\sigma^{p^\mathcal{T}} \cdot \boldsymbol{\nu}} = -\frac{\mathbf{K}_{f,\boldsymbol{\nu}}}{\mu} \left(\frac{p_{\sigma^+} - p_{\sigma^-}}{b_{f,\sigma}} - \rho \mathbf{g}\cdot\boldsymbol{\nu} \right) = -\frac{\mathbf{K}_{f,\boldsymbol{\nu}}}{\mu} \left(\frac{[\![p^\mathcal{T}]\!]_\sigma}{b_{f,\sigma}} - \rho \mathbf{g}\cdot\boldsymbol{\nu} \right). \tag{42}$$

If we sum up the above considerations, the finite volume scheme under study consists in the flux balance equations (35) and (40), together with the flux definitions (36), (37), (38) and (41), the definition (39) of the pressure fracture and the transmission condition (42).

4.3.2. *A priori estimates*

By using the various definitions given above of the discrete gradient operators, we can give a kind of variational formulation of the finite scheme under study.

Lemma 4.8 (Finite Volume variational formulation)**.** *Suppose we are given a solution $p^\mathcal{T} \in E(\mathcal{T})$ to the scheme* (35)-(42)*. Then, we have*

$$\frac{1}{2}\int_\Omega \frac{\mathbf{K}}{\mu}(\nabla^{\mathfrak{M},p^D} p^\mathcal{T} - \rho \Pi^\mathfrak{D} \mathbf{g}) \cdot \nabla^{\mathfrak{M},0} \phi^\mathcal{T}\, dx + \int_\Sigma \frac{\mathbf{K}_{f,\boldsymbol{\nu}}}{\mu} \left(\frac{[\![p^\mathcal{T}]\!]}{b_{f,\sigma}} - \rho \mathbf{g}\cdot\boldsymbol{\nu} \right) \frac{[\![\phi^\mathcal{T}]\!]}{b_{f,\sigma}} b_f(s)\, ds$$
$$- \int_\Sigma \overline{\phi^\mathcal{T}} [\![\mathbf{v}^{p^\mathcal{T}} \cdot \boldsymbol{\nu}]\!]\, ds = \int_\Omega Q \phi^\mathcal{T}\, dx, \quad \forall \phi^\mathcal{T} \in E(\mathcal{T}), \tag{43}$$

and

$$\int_\Sigma \frac{\mathbf{K}_{f,\boldsymbol{\tau}}}{\mu}(\nabla^{\mathfrak{S}}\Pi^{\mathfrak{S}}p^{\mathcal{T}} - \rho\mathbf{g}\cdot\boldsymbol{\tau})\nabla^{\mathfrak{S}}\phi^{\mathfrak{S}} b_f(s)\,ds = \int_\Sigma Q_f\phi^{\mathfrak{S}} b_f\,ds - \int_\Sigma [\![\mathbf{v}^{p^{\mathcal{T}}}\cdot\boldsymbol{\nu}]\!]\phi^{\mathfrak{S}}\,ds, \quad \forall \phi^{\mathfrak{S}} \in E(\mathfrak{S}). \tag{44}$$

Proof. Let us multiply equation (35) by ϕ_κ for all $\kappa \in \mathfrak{M}$ and sum over $\mathfrak{M}$. It follows

$$\sum_{\kappa\in\mathfrak{M}}\sum_{\sigma\in\mathcal{E}_\kappa} F_{\kappa,\sigma}\phi_\kappa = \sum_{\kappa\in\mathfrak{M}} m(\kappa)Q_\kappa\phi_\kappa.$$

We transform now the left-hand side as a sum over the set of edges. For edges $\sigma \in \mathcal{E}_{int}$ we use the conservativity of the fluxes and (36). For edges $\sigma \in \mathcal{E}^D_{ext}$ we use the definition (37) of the flux, and for edges $\sigma \in \mathfrak{S}$, we use the two definitions (38). We get

$$\begin{aligned}
\sum_{\kappa\in\mathfrak{M}} m(\kappa)Q_\kappa\phi_\kappa = &\sum_{\substack{\sigma\in\mathcal{E}_{int}\\ \sigma=\kappa|\mathcal{L}}} m(\sigma)\frac{\mathbf{K}}{\mu}\left(\frac{p_\mathcal{L}-p_\kappa}{d_{\kappa,\mathcal{L}}} - \rho\mathbf{g}\cdot\mathbf{n}_{\kappa,\mathcal{L}}\right)(\phi_\mathcal{L}-\phi_\kappa) + \sum_{\sigma\in\mathcal{E}^D_{ext}} m(\sigma)\frac{\mathbf{K}}{\mu}\left(\frac{p_\kappa - p^D_\sigma}{d_{\kappa,\sigma}} - \rho\mathbf{g}\cdot\mathbf{n}_\kappa\right)(\phi_\kappa - 0)\\
&+ \sum_{\sigma\in\mathfrak{S}} m(\sigma)\frac{\mathbf{K}}{\mu}\left(\frac{p_{\sigma^+} - p_{\kappa^+_\sigma}}{d_{\kappa^+_\sigma,\sigma}} - \rho\mathbf{g}\cdot\mathbf{n}^+\right)(\phi_{\sigma^+} - \phi_{\kappa^+_\sigma})\\
&+ \sum_{\sigma\in\mathfrak{S}} m(\sigma)\frac{\mathbf{K}}{\mu}\left(\frac{p_{\sigma^-} - p_{\kappa^-_\sigma}}{d_{\kappa^-_\sigma,\sigma}} - \rho\mathbf{g}\cdot\mathbf{n}^-\right)(\phi_{\sigma^-} - \phi_{\kappa^-_\sigma})\\
&+ \sum_{\sigma\in\mathfrak{S}} m(\sigma)\left(\phi_{\sigma^+}(\mathbf{v}^{p^{\mathcal{T}}}_{\sigma^+}\cdot\mathbf{n}^+) + \phi_{\sigma^-}(\mathbf{v}^{p^{\mathcal{T}}}_{\sigma^-}\cdot\mathbf{n}^-)\right).
\end{aligned}$$

Using (33), let us rewrite this expression as follows

$$\begin{aligned}
\sum_{\kappa\in\mathfrak{M}} m(\kappa)Q_\kappa\phi_\kappa = &\sum_{\substack{\sigma\in\mathcal{E}_{int}\\ \sigma=\kappa|\mathcal{L}}} m(\sigma)d_{\kappa,\mathcal{L}}\frac{\mathbf{K}}{\mu}\left(\frac{p_\mathcal{L}-p_\kappa}{d_{\kappa,\mathcal{L}}}\mathbf{n}_{\kappa,\mathcal{L}} - \rho(\mathbf{g}\cdot\mathbf{n}_{\kappa,\mathcal{L}})\mathbf{n}_{\kappa,\mathcal{L}}\right)\cdot\left(\frac{\phi_\mathcal{L}-\phi_\kappa}{d_{\kappa,\mathcal{L}}}\mathbf{n}_{\kappa,\mathcal{L}}\right)\\
&+ \sum_{\sigma\in\mathcal{E}^D_{ext}} m(\sigma)d_{\kappa,\sigma}\frac{\mathbf{K}}{\mu}\left(\frac{p_\kappa - p^D_\sigma}{d_{\kappa,\sigma}}\mathbf{n}_\kappa - \rho(\mathbf{g}\cdot\mathbf{n}_\kappa)\mathbf{n}_\kappa\right)\cdot\left(\frac{\phi_\kappa - 0}{d_{\kappa,\sigma}}\mathbf{n}_\kappa\right)\\
&+ \sum_{\sigma\in\mathfrak{S}} m(\sigma)d_{\kappa^+_\sigma,\sigma}\frac{\mathbf{K}}{\mu}\left(\frac{p_{\sigma^+} - p_{\kappa^+_\sigma}}{d_{\kappa^+_\sigma,\sigma}}\mathbf{n}^+ - \rho(\mathbf{g}\cdot\mathbf{n}^+)\mathbf{n}^+\right)\cdot\left(\frac{\phi_{\sigma^+} - \phi_{\kappa^+_\sigma}}{d_{\kappa^+_\sigma,\sigma}}\mathbf{n}^+\right)\\
&+ \sum_{\sigma\in\mathfrak{S}} m(\sigma)d_{\kappa^-_\sigma,\sigma}\frac{\mathbf{K}}{\mu}\left(\frac{p_{\sigma^-} - p_{\kappa^-_\sigma}}{d_{\kappa^-_\sigma,\sigma}}\mathbf{n}^- - \rho(\mathbf{g}\cdot\mathbf{n}^-)\mathbf{n}^-\right)\cdot\left(\frac{\phi_{\sigma^-} - \phi_{\kappa^-_\sigma}}{d_{\kappa^-_\sigma,\sigma}}\mathbf{n}^-\right)\\
&- \sum_{\sigma\in\mathfrak{S}} m(\sigma)\left([\![\phi^{\mathcal{T}}]\!]_\sigma\overline{\mathbf{v}^{p^{\mathcal{T}}}_\sigma\cdot\boldsymbol{\nu}} + \overline{\phi^{\mathcal{T}}_\sigma}[\![\mathbf{v}^{p^{\mathcal{T}}}_\sigma\cdot\boldsymbol{\nu}]\!]\right).
\end{aligned}$$

Since the mesh is conformal, notice that on any interior diamond cell $\mathcal{D}_\sigma \in \mathfrak{D}_{int}$ with $\sigma = \kappa|\mathcal{L}$, we have $m(\sigma)d_{\kappa,\mathcal{L}} = 2m(\mathcal{D}_\sigma)$, and for any boundary diamond cell $\mathcal{D}_\sigma \in \mathfrak{D}_{ext}$, we have $m(\sigma)d_{\kappa,\sigma} = 2m(\mathcal{D}_\sigma)$. Using now the transmission condition (42) and the definition 4.1 of the discrete gradient, (43) follows.

By similar, and in fact simpler, computations we obtain (44). ∎

Corollary 4.9. *Any solution $p^{\mathcal{T}} \in E(\mathcal{T})$ to the scheme (35)-(42) satisfies*

$$\int_\Omega Q\phi^{\mathcal{T}}\,dx + \int_\Sigma Q_f b_f \Pi^{\mathfrak{S}}\phi^{\mathcal{T}}\,ds = \frac{1}{2}\int_\Omega \frac{\mathbf{K}}{\mu}(\nabla^{\mathfrak{M},p^D}p^{\mathcal{T}} - \rho\Pi^{\mathfrak{D}}\mathbf{g})\cdot\nabla^{\mathfrak{M},0}\phi^{\mathcal{T}}\,dx$$
$$+\int_\Sigma \frac{\mathbf{K}_{f,\boldsymbol{\tau}}}{\mu}(\nabla^{\mathfrak{S}}\Pi^{\mathfrak{S}}p^{\mathcal{T}} - \rho\mathbf{g}\cdot\boldsymbol{\tau})\nabla^{\mathfrak{S}}\Pi^{\mathfrak{S}}\phi^{\mathcal{T}}\,ds + \int_\Sigma \frac{\mathbf{K}_{f,\boldsymbol{\nu}}}{\mu}\left(\frac{[\![p^{\mathcal{T}}]\!]}{b_{f,\sigma}} - \rho\mathbf{g}\cdot\boldsymbol{\nu}\right)\frac{[\![\phi^{\mathcal{T}}]\!]}{b_{f,\sigma}}b_f(s)\,ds$$
$$+\frac{(2\xi-1)\mu}{4\mathbf{K}_{f,\boldsymbol{\nu}}}\int_\Sigma b_f[\![\mathbf{v}^{p^{\mathcal{T}}}\cdot\boldsymbol{\nu}]\!][\![\mathbf{v}^{\phi^{\mathcal{T}}}\cdot\boldsymbol{\nu}]\!]\,ds, \quad \forall\phi^{\mathcal{T}}\in E(\mathcal{T}). \quad (45)$$

Hence, for any data, there exists a unique such solution $p^{\mathcal{T}} \in E(\mathcal{T})$ and there exists $C>0$ which only depends only on the data $\mu, \rho, \mathbf{K}, \mathbf{K}_{f,\boldsymbol{\tau}}, \mathbf{K}_{f,\boldsymbol{\nu}}, \Omega, b_f$ and $\mathrm{reg}(\mathcal{T})$ such that we have

$$\|p^{\mathcal{T}}\|_{W^{\mathcal{T}},p^D} \le C\left(\|Q\|_{0,\Omega} + \|Q_f\|_{0,\Sigma} + \|p^D\|_{\frac{1}{2},\Gamma_D} + |\mathbf{g}|\right). \quad (46)$$

Proof. We obtain (45) by taking $\phi^{\mathfrak{S}} = \Pi^{\mathfrak{S}}\phi^{\mathcal{T}}$ in (44) and adding it to (43).

There exists $R \in H^1(\Omega)$ an extension of p^D compactly supported in $\overline{\Omega}\setminus\Sigma$, and such that $\|R\|_{1,\Omega} \le C(\Omega)\|p^D\|_{\frac{1}{2},\Gamma_D}$. We introduce the projection $R^{\mathcal{T}} \in E(\mathcal{T})$ of R on the mesh $\mathcal{T}$, which reads $R^{\mathcal{T}} = (R^{\mathfrak{M}}, \gamma_{0,N}R^{\mathcal{T}}, \gamma^+R^{\mathcal{T}}, \gamma^-R^{\mathcal{T}})$ with $R^{\mathfrak{M}} = (R_\kappa)_{\kappa\in\mathfrak{M}}$ the mean value projection of R on the mesh $\mathfrak{M}$ that is R_κ is the mean-value of R on the ball $B(x_\kappa, r_\kappa)$ defined in Section 4.1. We naturally choose to take $\gamma^+R^{\mathcal{T}} = \gamma^-R^{\mathcal{T}} = 0$ since R vanishes in the neighborhood of the fracture Σ, and we take $R_\sigma = \frac{1}{m(\sigma)}\int_\sigma R\,ds$ for any $\sigma \in \mathcal{E}^N_{ext}$.

We can prove as in [2,12] that

$$\|\nabla^{\mathfrak{M},p^D}R^{\mathcal{T}}\|_{0,\Omega} \le C(\Omega,\mathrm{reg}(\mathcal{T}))\|R\|_{1,\Omega} \le C\|p^D\|_{\frac{1}{2},\Gamma_D}.$$

We remark that, if $\mathrm{size}(\mathcal{T})$ is small enough, then $[\![\mathbf{v}^{R^{\mathcal{T}}}\cdot\boldsymbol{\nu}]\!] = \Pi^{\mathfrak{S}}R^{\mathfrak{M}} = 0$. Hence, taking $\phi^{\mathcal{T}} = p^{\mathcal{T}} - R^{\mathcal{T}}$ in (45), we obtain

$$\frac{1}{2}\int_\Omega \frac{\mathbf{K}}{\mu}(\nabla^{\mathcal{T},p^D}p^{\mathcal{T}} - \rho\Pi^{\mathfrak{D}}\mathbf{g})\cdot(\nabla^{\mathfrak{M},p^D}p^{\mathcal{T}} - \nabla^{\mathfrak{M},p^D}R^{\mathcal{T}})\,dx + \int_\Sigma \frac{\mathbf{K}_{f,\boldsymbol{\tau}}}{\mu}(\nabla^{\mathfrak{S}}\Pi^{\mathfrak{S}}p^{\mathcal{T}} - \rho\mathbf{g}\cdot\boldsymbol{\tau})\cdot\nabla^{\mathfrak{S}}\Pi^{\mathfrak{S}}p^{\mathcal{T}}b_f(s)\,ds$$
$$+\int_\Sigma \frac{\mathbf{K}_{f,\boldsymbol{\nu}}}{\mu}\left(\frac{[\![p^{\mathcal{T}}]\!]}{b_{f,\sigma}} - \rho\mathbf{g}\cdot\boldsymbol{\nu}\right)\frac{[\![p^{\mathcal{T}}]\!]}{b_{f,\sigma}}b_f(s)\,ds + \frac{(2\xi-1)\mu}{4\mathbf{K}_{f,\boldsymbol{\nu}}}\int_\Sigma [\![\mathbf{v}^{p^{\mathcal{T}}}\cdot\boldsymbol{\nu}]\!]^2 b_f(s)\,ds$$
$$= \int_\Omega Q(x)(p^{\mathfrak{M}} - R^{\mathfrak{M}})(x)\,dx + \int_\Sigma Q_f(s)\Pi^{\mathfrak{S}}p^{\mathcal{T}}(s)b_f(s)\,ds$$

We deduce by using Cauchy-Schwarz's and Young's inequalities that

$$\|p^{\mathcal{T}}\|^2_{W^{\mathcal{T}},p^D} \le C\left(\|Q\|_{0,\Omega}\|p^{\mathfrak{M}} - R^{\mathfrak{M}}\|_{0,\Omega} + \|R^{\mathcal{T}}\|^2_{1,\mathcal{T}} + \|Q_f\|_{0,\Sigma}\|\Pi^{\mathfrak{S}}p^{\mathcal{T}}\|_{0,\Sigma}\right)$$

The estimate (46) follows immediately using the trace Lemma 4.6 and the Poincaré inequality (Lemma 4.7).

Finally, applying (46) for $p^D = Q = Q_f = 0$ and $\mathbf{g} = 0$, we find, using Poincaré Lemma 4.7, that this implies $p^{\mathcal{T}} = 0$. Since the discrete system is a square linear system we obtain existence and uniqueness of the solution for any data. ∎

4.4. **Convergence of the numerical scheme**

4.4.1. *Compactness properties*

Lemma 4.10 (Compactness Lemma in Ω)**.** *Let $(\mathcal{T}_n)_n$ be a family of meshes such that $size(\mathcal{T}_n) \underset{n\to\infty}{\longrightarrow} 0$ and $(\mathrm{reg}(\mathcal{T}_n))_n$ is bounded.*

Suppose now given a family of discrete pressure fields $p^{\mathcal{T}_n} = (p^{\mathfrak{M}_n}, \gamma_{0,N} p^{\mathcal{T}_n}, \gamma^{\pm} p^{\mathcal{T}_n}) \in E(\mathcal{T}_n)$ such that $(\|p^{\mathcal{T}_n}\|_{1,\mathcal{T}_n})_n$ is bounded. Then there exists $p \in H^1(\Omega)$ with $\gamma_{0,D} p = p^D$ and such that, up to a subsequence still denoted by $(p^{\mathcal{T}_n})_n$, we have

$$p^{\mathfrak{M}_n} \xrightarrow[n\to\infty]{} p \text{ strongly in } L^2(\Omega) \tag{47}$$

$$\nabla^{\mathfrak{M}_n, p^D} p^{\mathcal{T}_n} \xrightarrow[n\to\infty]{} \nabla p \text{ weakly in } (L^2(\Omega))^2 \tag{48}$$

$$\gamma^{\pm} p^{\mathcal{T}_n} \xrightarrow[n\to\infty]{} \gamma^{\pm} p \text{ weakly in } L^2(\Sigma) \tag{49}$$

$$[\![p^{\mathcal{T}_n}]\!] \xrightarrow[n\to\infty]{} [\![p]\!] \text{ weakly in } L^2(\Sigma) \tag{50}$$

$$\gamma_{0,D} p^{\mathfrak{M}_n} \xrightarrow[n\to\infty]{} p^D \text{ strongly in } L^2(\Gamma_D) \tag{51}$$

$$\gamma_{0,N} p^{\mathfrak{M}_n} \xrightarrow[n\to\infty]{} \gamma_{0,N} p \text{ weakly in } L^2(\Gamma_N) \tag{52}$$

Proof.

- **First step.**

We first prove that the family $(p^{\mathfrak{M}_n})_n$ is relatively compact in $L^2(\Omega)$ using Kolmogoroff Theorem. To this end, we classically introduce $\widetilde{p^{\mathfrak{M}_n}}$, the extension by 0 of $p^{\mathfrak{M}_n}$ on $\mathbb{R}^2 \setminus \Omega$. It is clear that the assumption implies that $(\widetilde{p^{\mathfrak{M}_n}})_n$ is bounded in $L^2(\mathbb{R}^2)$.

We now prove, using similar methods than in [12], that there exists $C > 0$ such that for all $|\eta| < 1$, we have $\|\widetilde{p^{\mathfrak{M}_n}}(\cdot + \eta) - \widetilde{p^{\mathfrak{M}_n}}(\cdot)\|^2_{0,\mathbb{R}^2} \leq C|\eta|$. To this end, we define for all $\sigma \in \mathcal{E}$, the function χ_σ from $\mathbb{R}^2 \times \mathbb{R}^2$ to $\{0,1\}$ by $\chi_\sigma(x,y) = 1$ if $[x,y] \cap \sigma \neq \emptyset$ and $\chi_\sigma(x,y) = 0$ else. Note also $c_\sigma = \left| \mathbf{n}_\sigma \cdot \frac{\eta}{|\eta|} \right|$ for any edge σ. Finally, notice that if $c_\sigma = 0$ then $\chi_\sigma(x, x+\eta) = 0$ for almost every $x \in \Omega$.

Hence, for almost every $x \in \Omega$ we have

$$\begin{aligned} |\widetilde{p^{\mathfrak{M}_n}}(x+\eta) - \widetilde{p^{\mathfrak{M}_n}}(x)| \leq & \sum_{\substack{\sigma \in \mathcal{E}_{int} \\ \sigma = \mathcal{K}|\mathcal{L}}} \chi_\sigma(x, x+\eta) |p_\mathcal{K} - p_\mathcal{L}| + \sum_{\sigma \in \mathcal{E}_{ext}} \chi_\sigma(x, x+\eta) |p_{\mathcal{K}_\sigma}| \\ & + \sum_{\sigma \in \mathfrak{S}} \chi_\sigma(x, x+\eta) \left(|p_{\mathcal{K}_\sigma^+} - p_{\sigma^+}| + |p_{\mathcal{K}_\sigma^-} - p_{\sigma^-}| + |p_{\sigma^+} - p_{\sigma^-}| \right). \end{aligned}$$

Using the Cauchy-Schwarz inequality, it follows

$$\begin{aligned} |\widetilde{p^{\mathfrak{M}_n}}(x+\eta) - \widetilde{p^{\mathfrak{M}_n}}(x)|^2 \leq & C \left(\sum_{\substack{\sigma \in \mathcal{E}_{int} \\ \sigma = \mathcal{K}|\mathcal{L}}} \chi_\sigma(x, x+\eta) \frac{|p_\mathcal{K} - p_\mathcal{L}|^2}{c_\sigma d_\sigma} \right) \times \left(\sum_{\sigma \in \mathcal{E}_{int}} \chi_\sigma(x, x+\eta) c_\sigma d_\sigma \right) \\ & + C \left(\sum_{\sigma \in \mathcal{E}_{ext}} \chi_\sigma(x, x+\eta) \frac{|p_{\mathcal{K}_\sigma}|^2}{c_\sigma} \right) \times \left(\sum_{\sigma \in \mathcal{E}_{ext}} \chi_\sigma(x, x+\eta) c_\sigma \right) \\ & + C \left(\sum_{\sigma \in \mathfrak{S}} \chi_\sigma(x, x+\eta) \frac{|p_{\mathcal{K}_\sigma^+} - p_{\sigma^+}|^2}{c_\sigma d_{\mathcal{K}_\sigma^+}} \right) \times \left(\sum_{\sigma \in \mathfrak{S}} \chi_\sigma(x, x+\eta) c_\sigma d_{\mathcal{K}_\sigma^+} \right) \\ & + C \left(\sum_{\sigma \in \mathfrak{S}} \chi_\sigma(x, x+\eta) \frac{|p_{\mathcal{K}_\sigma^-} - p_{\sigma^-}|^2}{c_\sigma d_{\mathcal{K}_\sigma^-}} \right) \times \left(\sum_{\sigma \in \mathfrak{S}} \chi_\sigma(x, x+\eta) c_\sigma d_{\mathcal{K}_\sigma^-} \right) \\ & + C \left(\sum_{\sigma \in \mathfrak{S}} \chi_\sigma(x, x+\eta) \frac{|p_{\sigma^+} - p_{\sigma^-}|^2}{c_\sigma {b_{f,\sigma}}^2} \right) \times \left(\sum_{\sigma \in \mathfrak{S}} \chi_\sigma(x, x+\eta) c_\sigma {b_{f,\sigma}}^2 \right). \end{aligned} \tag{53}$$

It is proved in [12] that, there exists $C>0$ such that for any $x\in\Omega$ we have

$$\sum_{\sigma\in\mathcal{E}_{int}}\chi_\sigma(x,x+\eta)c_\sigma d_\sigma\le|\eta|+Csize(\mathcal{T}_n),\ \sum_{\sigma\in\mathcal{E}_{ext}}\chi_\sigma(x,x+\eta)c_\sigma d_\sigma\le C.$$

By exactly the same computations it follows that for any $x\in\Omega$ we have

$$\sum_{\sigma\in\mathcal{E}_\Sigma}\chi_\sigma(x,x+\eta)d_{\mathcal{K}_\sigma^+,\sigma}c_\sigma+\sum_{\sigma\in\mathcal{E}_\Sigma}\chi_\sigma(x,x+\eta)d_{\mathcal{K}_\sigma^-,\sigma}c_\sigma\le|\eta|+Csize(\mathcal{T}_n),$$

and moreover, since we assumed here that Σ is a segment (or even a finite number N_Σ of connected straight lines) we have for any $x\in\Omega$

$$\sum_{\sigma\in\mathcal{E}_\Sigma}\chi_\sigma(x,x+\eta)b_f^2c_\sigma\le N_\Sigma\|b_f\|^2_{\infty,\Sigma}.$$

We use now these bounds in (53), then we integrate the inequality with respect to $x\in\Omega$. Noting that

$$\int_{\mathbb{R}^2}\chi_\sigma(x,x+\eta)\,dx\le m(\sigma)c_\sigma|\eta|,\quad\forall\sigma,\,\forall\eta,$$

we get, using in particular the trace Lemma 4.6, the estimate

$$\begin{aligned}\|\widetilde{p^{\mathfrak{M}_n}}(\cdot+\eta)-\widetilde{p^{\mathfrak{M}_n}}(\cdot)\|^2_{0,\mathbb{R}^2}\le&C(|\eta|+\mathrm{size}(\mathcal{T}_n))|\eta|\left(\sum_{\substack{\sigma\in\mathcal{E}_{int}\\ \sigma=\mathcal{K}|\mathcal{L}}}m(\mathcal{D}_\sigma)\left|\frac{p_\mathcal{K}-p_\mathcal{L}}{d_{\mathcal{K},\mathcal{L}}}\right|^2\right)\\&+C(|\eta|+\mathrm{size}(\mathcal{T}_n))|\eta|\left(\sum_{\sigma\in\mathfrak{S}}m(\mathcal{D}_{\sigma^\pm})\left|\frac{p_{\mathcal{K}_\sigma^\pm}-p_{\sigma^\pm}}{d_{\mathcal{K}_\sigma^\pm}}\right|^2\right)\\&+C|\eta|\left(\sum_{\sigma\in\mathcal{E}_{ext}}m(\sigma)|p_{\mathcal{K}_\sigma}|^2\right)+C|\eta|\left(\sum_{\sigma\in\mathfrak{S}}m(\sigma)\left|\frac{p_{\sigma^+}-p_{\sigma^-}}{b_{f,\sigma}}\right|^2\right)\\\le&C|\eta|\|p^{\mathcal{T}_n}\|^2_{1,\mathcal{T}_n}\le C'|\eta|.\end{aligned}$$

Hence, by the Kolmogoroff theorem, the sequence $(p^{\mathfrak{M}_n})_n$ is compact, and then converges in $L^2(\Omega)$, up to a subsequence. Let us denote by p its limit.

- **Second Step.** We have

$$\begin{aligned}\|\gamma_{0,D}p^{\mathfrak{M}_n}-p^D\|^2_{0,\Gamma_D}&\le2\sum_{\sigma\in\mathcal{E}_{ext}^D}m(\sigma)|p_{\mathcal{K}_\sigma}-p_\sigma^D|^2+2\sum_{\sigma\in\mathcal{E}_{ext}^D}\int_\sigma|p^D(s)-p_\sigma^D|^2\,ds\\&\le C\sum_{\sigma\in\mathcal{E}_{ext}^D}d_{\mathcal{K}_\sigma,\sigma}m(\mathcal{D}_\sigma)\left|\frac{p_{\mathcal{K}_\sigma}-p_\sigma^D}{d_{\mathcal{K}_\sigma,\sigma}}\right|^2+C\sum_{\sigma\in\mathcal{E}_{ext}^D}m(\sigma)\int_\sigma\int_\sigma\left|\frac{p^D(s)-p^D(t)}{|s-t|}\right|^2ds\,dt\\&\le C\mathrm{size}(\mathcal{T}_n)\left(\|p^{\mathcal{T}_n}\|^2_{1,\mathcal{T}_n}+\|p^D\|^2_{\frac12,\Gamma_D}\right).\end{aligned}$$

Hence we obtain the strong L^2 convergence of the trace $\gamma_{0,D}p^{\mathfrak{M}_n}$ towards the boundary data p^D.

- **Third step.** The bound $\|p^{\mathcal{T}_n}\|_{1,\mathcal{T}} \leq C$ and the trace Lemma 4.6 give that there exists $G \in (L^2(\Omega))^2$, $q^+ \in L^2(\Sigma)$, $q^- \in L^2(\Sigma)$, $q_N \in L^2(\Gamma_N)$, $q_D \in L^2(\Gamma_D)$ such that up to a subsequence, we have

$$\begin{aligned} \nabla^{\mathfrak{M}_n,p^D} p^{\mathcal{T}_n} &\xrightarrow[n\to\infty]{} G \text{ weakly in } L^2(\Omega), \\ \gamma^{\pm} p^{\mathcal{T}_n} &\xrightarrow[n\to\infty]{} q^{\pm} \text{ weakly in } L^2(\Sigma), \\ \gamma_{0,N} p^{\mathfrak{M}_n} &\xrightarrow[n\to\infty]{} q_N \text{ weakly in } L^2(\Gamma_N). \end{aligned}$$

Let us now identify the functions $G, q^{\pm}$ and q_N. To this end, for any $\Phi \in \mathcal{S}^2$ ($\mathcal{S}$ being defined in (14)), let us write

$$\int_\Omega p^{\mathfrak{M}} \nabla \cdot \Phi \, dx + \int_\Omega \nabla^{\mathfrak{M},p^D} p^{\mathcal{T}} \cdot \Phi \, dx = \sum_{\mathcal{K}\in\mathcal{T}} p_{\mathcal{K}} \sum_{\sigma\in\mathcal{E}_{\mathcal{K}}} \int_\sigma \Phi_{|\mathcal{K}} \cdot \mathbf{n}_{\mathcal{K},\sigma} \, ds + \sum_{\mathcal{D}\in\mathfrak{D}} \nabla^{\mathfrak{M},p^D} p^{\mathcal{T}} \cdot \left(\int_{\mathcal{D}} \Phi \, dx \right)$$

Noting that $\nabla^{\mathfrak{M},p^D} p^{\mathcal{T}_n}$ is parallel to $\mathbf{n}_{\mathcal{K},\sigma}$ on any diamond cell, it follows that

$$\nabla^{\mathfrak{M},p^D} p^{\mathcal{T}_n} \cdot \left(\int_{\mathcal{D}} \Phi \, dx \right) = \nabla^{\mathfrak{M},p^D} p^{\mathcal{T}_n} \cdot \left(\int_{\mathcal{D}} \Phi \cdot \mathbf{n}_{\mathcal{K},\sigma} \right) \mathbf{n}_{\mathcal{K},\sigma}.$$

Hence, reordering the first sum above as a sum over the diamond cells we derive that

$$\begin{aligned} &\int_\Omega p^{\mathfrak{M}_n} \nabla \cdot \Phi \, dx + \int_\Omega \nabla^{\mathfrak{M}_n,p^D} p^{\mathcal{T}_n} \cdot \Phi \, dx \\ &\qquad = \sum_{\mathcal{D}\in\mathfrak{D}} m(\mathcal{D}) \nabla^{\mathfrak{M}_n,p^D} p^{\mathcal{T}_n} \cdot \left(\frac{1}{m(\mathcal{D})} \int_{\mathcal{D}} \Phi \cdot \mathbf{n}_{\mathcal{K},\sigma} \, dx - \frac{1}{m(\sigma)} \int_\sigma \Phi \cdot \mathbf{n}_{\mathcal{K},\sigma} \, ds \right) \mathbf{n}_{\mathcal{K},\sigma} \\ &+ \sum_{\sigma\in\mathcal{E}^D_{ext}} p^D_\sigma \int_\sigma \Phi \cdot \mathbf{n} \, ds + \sum_{\sigma\in\mathcal{E}^N_{ext}} \int_\sigma \gamma_{0,N} p^{\mathfrak{M}_n} \Phi \cdot \mathbf{n} \, ds + \sum_{\sigma\in\mathfrak{S}} \int_\sigma \left(\gamma^+ p^{\mathcal{T}_n} \left(\gamma^+\Phi\right) \cdot \mathbf{n}^+ + \gamma^- p^{\mathcal{T}_n} \left(\gamma^-\Phi\right) \cdot \mathbf{n}^- \right) ds. \end{aligned} \tag{54}$$

By using Taylor expansions, we easily see that for any diamond cell in the domain we have

$$\left| \frac{1}{m(\mathcal{D})} \int_{\mathcal{D}} \Phi \, dx - \frac{1}{m(\sigma)} \int_\sigma \Phi \, ds \right| \leq C \text{size}(\mathcal{T}_n) \|\Phi\|_{\mathcal{S}^2}.$$

It follows that the first term in the right-hand side of (54) tends to 0 when $n \to \infty$. Passing to the limit in the other terms gives

$$\int_\Omega p \nabla \cdot \Phi \, dx + \int_\Omega G \cdot \Phi \, dx = \int_{\Gamma_D} p^D \Phi \cdot \mathbf{n} \, ds + \int_{\Gamma_N} q_N \Phi \cdot \mathbf{n} \, ds + \int_\Sigma \left(q^+ \left(\gamma^+\Phi\right) \cdot \mathbf{n}^+ + q^- \left(\gamma^-\Phi\right) \cdot \mathbf{n}^- \right) ds.$$

We conclude that $p \in H^1(\Omega)$ and $G = \nabla p$, $\gamma_{0,D} p = p^D$, $q_N = \gamma_{0,N} p$, $q^{\pm} = \gamma^{\pm} p$ and the claim is proved. □

As a consequence to this result, we deduce a weak convergence result of the projection of the gravity term, as defined in Definition 4.2.

Corollary 4.11. *For any family of meshes $(\mathcal{T}_n)_n$ like in the previous Lemma we have*

$$\Pi^{\mathfrak{D}_n} \mathbf{g} \xrightarrow[n\to\infty]{} \mathbf{g}, \quad \textit{weakly in } (L^2(\Omega))^2.$$

Proof. Notice that $\mathbf{g}$ is the gradient of the map $p(x) = (\mathbf{g}, x)$. Let $p^D = p_{|\Gamma_D}$ and introduce

$$p^{\mathcal{T}_n} = (p^{\mathfrak{M}_n} = (p(x_\mathcal{K}))_\mathcal{K}, \gamma_{0,N} p^{\mathcal{T}_n} = (p(x_\sigma))_{\sigma \in \mathcal{E}_{ext}^N}, \gamma^+ p^{\mathcal{T}_n} = (p(x_\sigma))_{\sigma \in \mathfrak{S}}, \gamma^- p^{\mathcal{T}_n} = (p(x_\sigma))_{\sigma \in \mathfrak{S}}).$$

It is easily seen that $\Pi^{\mathfrak{D}_n} \mathbf{g} = \nabla^{\mathfrak{M}_n, p^D} p^{\mathcal{T}_n}$, and that a bound $\|p^{\mathcal{T}_n}\|_{1,\mathcal{T}_n} \leq C|\mathbf{g}|$ holds. By using the previous Lemma we have the weak convergence of a subsequence of $(\Pi^{\mathfrak{D}_n} \mathbf{g})_n$ towards $\nabla p = \mathbf{g}$. The convergence of the complete sequence is then proved since the limit $\mathbf{g}$ does not depend on the subsequence. □

We can also obtain by similar and simpler arguments a 1D compactness result on the fracture Σ that we state here.

Lemma 4.12 (Compactness lemma in Σ)**.** *Let $(\mathcal{T}_n)_n$ be a family of meshes such that size$(\mathcal{T}_n) \underset{n\to\infty}{\longrightarrow} 0$ and $(\mathrm{reg}(\mathcal{T}_n))_n$ is bounded. Let now $p^{\mathfrak{S}_n} \in E(\mathfrak{S}_n)$ be a family of fracture pressure fields such that $(\|p^{\mathfrak{S}_n}\|_{1,b_f,\mathfrak{S}_n})_n$ is bounded. Then, there exists $p_f \in H^1(\Sigma)$ such that, up to a subsequence still denoted by $p^{\mathfrak{S}_n}$, we have*

$$\begin{aligned} p^{\mathfrak{S}_n} &\xrightarrow[n\to\infty]{} p_f \text{ strongly in } L^2(\Sigma), \\ \nabla^{\mathfrak{S}_n} p^{\mathfrak{S}_n} &\xrightarrow[n\to\infty]{} \nabla_{\boldsymbol{\tau}} p_f \text{ weakly in } L^2(\Sigma). \end{aligned}$$

4.4.2. *Convergence theorem*

We are now in position to prove the main result of this paper, which shows the convergence of the finite volume scheme towards a solution of our asymptotic model of flows in fractured porous media.

Theorem 4.13. *Let $(\mathcal{T}_n)_n$ be a family of meshes such that* size$(\mathcal{T}_n) \xrightarrow[n\to\infty]{} 0$ *and $(\mathrm{reg}(\mathcal{T}_n))_n$ is bounded. Then, the unique solution $p^{\mathcal{T}_n}$ to the scheme* (35)-(42) *for the mesh $\mathcal{T}_n$ converges towards the unique solution $p \in \mathcal{W}$ of problem* (19)-(24)*.*

More precisely, $(p^{\mathfrak{M}_n})_n$ strongly converges towards p in $L^2(\Omega)$, $(\nabla^{\mathfrak{M}_n, p^D} p^{\mathfrak{M}_n})_n$ weakly converges towards ∇p in $(L^2(\Omega))^2$, $(\Pi^{\mathfrak{S}_n} p^{\mathcal{T}_n})_n$ strongly converges towards $\Pi_f p$ in $L^2(\Sigma)$ and $(\nabla^{\mathfrak{S}_n} \Pi^{\mathfrak{S}_n} p^{\mathcal{T}_n})_n$ weakly converges towards $\nabla^{\mathfrak{S}} \Pi_f p$ in $L^2(\Sigma)$.

Proof. Notice that we are going to show the convergence of a subsequence which is enough to prove the claim since we already know that the solution to (19)-(24) is unique.

- From the a priori estimate obtained in Lemma 4.9, and the compactness Lemmas 4.10 and 4.12, we obtain that there exists $p \in H^1(\Omega)$ and $p_f \in H^1(\Sigma)$ such that the convergences (47)-(52) hold and moreover

$$\Pi^{\mathfrak{S}_n} p^{\mathcal{T}_n} \xrightarrow[n\to\infty]{} p_f \text{ strongly in } L^2(\Sigma) \tag{55}$$

$$\nabla^{\mathfrak{S}_n} \Pi^{\mathfrak{S}_n} p^{\mathcal{T}_n} \xrightarrow[n\to\infty]{} \nabla_{\boldsymbol{\tau}} p_f \text{ weakly in } L^2(\Sigma). \tag{56}$$

  We want now to show that $p_f = \Pi_f p$, that $p \in \mathcal{W}$ and that it is a solution to (19)-(24).
- From equation (42) and (50) we derive that

$$\overline{\mathbf{v}^{p^{\mathcal{T}_n}} \cdot \boldsymbol{\nu}} \xrightarrow[n\to+\infty]{} -\frac{\mathbf{K}_{f,\boldsymbol{\nu}}}{\mu} \left(\frac{[\![p]\!]}{b_f} - \rho \mathbf{g} \cdot \boldsymbol{\nu} \right) \quad \text{weakly in } L^2(\Sigma).$$

  From now on, we need to perform a separate analysis for the two cases $\xi > \frac{1}{2}$ and $\xi = \frac{1}{2}$, since in the first case we have an additional *a priori* estimate and we have to pass to the limit independently in the problem in the porous matrix and in the fracture, whereas in the second case we must treat simultaneously the two equations.
- **The case $\xi > \frac{1}{2}$**

– Thanks to the *a priori* estimate (46) and the definition (34) of the norm $\|\cdot\|_{W^{\mathcal{T}},p^D}$, we see that for $\xi > \frac{1}{2}$, the quantity $[\![\mathbf{v}^{p^{\mathcal{T}_n}} \cdot \boldsymbol{\nu}]\!]$ is bounded in $L^2_{b_f}(\Sigma)$. Hence, there exists $\Psi \in L^2(\Sigma)$ such that, up to a subsequence,

$$[\![\mathbf{v}^{p^{\mathcal{T}_n}} \cdot \boldsymbol{\nu}]\!] \xrightarrow[n\to\infty]{} \Psi \text{ weakly in } L^2(\Sigma). \tag{57}$$

Notice that, thanks to assumptions (16), it is easily seen that $\sum_{\sigma\in\mathfrak{S}_n} \mathbb{1}_\sigma b_{f,\sigma}$ converges strongly towards b_f in $L^2(\Sigma)$ for instance. Hence, we can pass to the limit in equation (39) and find

$$p_f = \frac{1}{2}(\gamma^+ p + \gamma^- p) + \frac{(2\xi-1)\mu}{4\mathbf{K}_{f,\boldsymbol{\nu}}} b_f \Psi. \tag{58}$$

– Let now ϕ_f be a function in $\mathcal{C}^2(\Sigma)$, which is constant near the two ends $\partial\Sigma^+$ and $\partial\Sigma^-$ of Σ. Let us take $\phi^{\mathfrak{S}} = ((\phi_f(x_\sigma))_\sigma, \phi_f(\partial\Sigma^-), \phi_f(\partial\Sigma^+)) \in E(\mathfrak{S})$ in (44). It follows that, for n large enough (so that ϕ_f is constant on the two edges σ touching the boundary of Σ) we have

$$\begin{aligned}\int_\Sigma \frac{\mathbf{K}_{f,\boldsymbol{\tau}}}{\mu}(\nabla^{\mathfrak{S}_n}\Pi^{\mathfrak{S}_n} p^{\mathcal{T}_n} - \rho\mathbf{g}\cdot\boldsymbol{\tau})(\nabla_{\boldsymbol{\tau}}\phi_f(s) + R_n(s))b_f(s)\,ds \\ = \int_\Sigma Q_f(s)(\phi_f(s)+r_n(s))b_f(s)\,ds - \int_\Sigma [\![\mathbf{v}^{p^{\mathcal{T}_n}}\cdot\boldsymbol{\nu}]\!](\phi_f(s)+r_n(s))\,ds,\end{aligned} \tag{59}$$

where

$$R_n(s) = \frac{\phi_f(x_{\sigma'}) - \phi_f(x_\sigma)}{d_{\sigma,\sigma'}}(\boldsymbol{\tau}_{\sigma,\sigma'}\cdot\boldsymbol{\tau}) - \nabla_{\boldsymbol{\tau}}\phi_f(s), \quad \forall s \in S_e, \forall e = \sigma|\sigma' \in \mathfrak{V}_{int},$$

$$R_n(s) = 0, \quad \forall s \in S_e, \forall e \in \{\partial\Sigma^-, \partial\Sigma^+\},$$

and

$$r_n(s) = \phi_f(x_\sigma) - \phi_f(s), \ \forall s \in \sigma, \forall \sigma \in \mathfrak{S}_n.$$

Since ϕ_f is smooth, we easily see that $\|R_n\|_{\infty,\Sigma} + \|r_n\|_{\infty,\Sigma} \le \mathrm{size}(\mathcal{T}_n)\|\phi_f\|_{\mathcal{C}^2}$. Hence, we can pass to the limit in (59) by using (56) and (57). We find that p_f solves

$$-\nabla_{\boldsymbol{\tau}}\left(b_f(s)\frac{\mathbf{K}_{f,\boldsymbol{\tau}}}{\mu}(\nabla_{\boldsymbol{\tau}}p_f - \rho\mathbf{g}\cdot\boldsymbol{\tau})\right) = b_f Q_f - \Psi \text{ on } \Sigma, \tag{60}$$

as well as the Neumann boundary condition on $\partial\Sigma$.

– Let $\phi \in \mathcal{S}$ (see the definition (14)) such that $\phi = 0$ on Γ_D. We use here the center-valued projection $\Pi^{\mathcal{T}_n,c}\phi = (\Pi^{\mathfrak{M}_n,c}\phi, \gamma_{0,N}\Pi^{\mathcal{T}_n,c}\phi, \gamma^\pm\Pi^{\mathcal{T}_n,c}\phi)$ of ϕ on the mesh $\mathcal{T}_n$ defined by

$$\begin{cases} \Pi^{\mathfrak{M}_n,c}\phi = (\phi_\kappa)_{\kappa\in\mathfrak{M}_n},\ \phi_\kappa = \phi(x_\kappa), \\ \gamma^\pm\Pi^{\mathcal{T}_n,c}\phi = (\phi_{\sigma^\pm})_{\sigma\in\mathfrak{S}_n},\ \phi_{\sigma^\pm} = \gamma^\pm\phi(x_\sigma), \\ \gamma_{0,N}\Pi^{\mathcal{T}_n,c}\phi = (\phi^N_\sigma)_{\sigma\in\mathcal{E}^N_{ext}},\ \phi^N_\sigma = \gamma_{0,N}\phi(x_\sigma). \end{cases}$$

It follows from (43) that

$$\sum_{\mathcal{D}\in\mathfrak{D}}\int_{\mathcal{D}}\frac{\mathbf{K}}{\mu}\left(\nabla^{\mathfrak{M}_n,p^D}p^{\mathcal{T}_n}-\rho\Pi^{\mathfrak{D}_n}\mathbf{g}\right)\cdot\left((\nabla\phi(x)\cdot\mathbf{n}_\sigma+\widetilde{R}_n(x))\,\mathbf{n}_\sigma\right)dx$$
$$+\int_\Sigma\frac{\mathbf{K}_{f,\boldsymbol{\nu}}}{\mu}\left(\frac{[\![p^{\mathcal{T}_n}]\!]}{b_{f,\sigma}}-\rho\mathbf{g}\cdot\boldsymbol{\tau}\right)\left(\frac{[\![\phi]\!]+r_n^+-r_n^-}{b_{f,\sigma}}\right)b_f\,ds-\int_\Sigma\left(\overline{\phi}+\frac{r_n^++r_n^-}{2}\right)[\![\mathbf{v}^{p^{\mathcal{T}_n}}\cdot\boldsymbol{\nu}]\!]\,ds$$
$$=\int_\Omega Q(x)\Pi^{\mathfrak{M}_n,c}\phi\,dx,\quad(61)$$

where

$$\widetilde{R}_n(x)=\nabla\phi(x)\cdot\mathbf{n}_\sigma-\nabla^{\mathfrak{M}_n,0}\Pi^{\mathcal{T}_n,c}\phi\cdot\mathbf{n}_\sigma,\ \forall x\in\mathcal{D}_\sigma,\forall\mathcal{D}_\sigma\in\mathfrak{D},$$
$$r_n^\pm(s)=\gamma^\pm\phi(x_\sigma)-\gamma^\pm\phi(s),\forall s\in\sigma\in\mathfrak{S}_n.$$

Since ϕ is smooth and vanishes on Γ_D, we easily get that

$$\|\widetilde{R}_n\|_{\infty,\Omega}+\|r_n^\pm\|_{\infty,\Sigma}\le C\,\mathrm{size}(\mathcal{T}_n)\|\phi\|_{\mathcal{S}}.$$

Furthermore, on each diamond cell the vector $\nabla^{\mathfrak{M}_n,p^D}p^{\mathcal{T}_n}$ is parallel to $\mathbf{n}_\sigma$. Hence we get

$$\int_{\mathcal{D}}\nabla^{\mathfrak{M}_n,p^D}p^{\mathcal{T}_n}\cdot\left((\nabla\phi(x)\cdot\mathbf{n}_\sigma)\,\mathbf{n}_\sigma\right)dx=\int_{\mathcal{D}}\nabla^{\mathfrak{M}_n,p^D}p^{\mathcal{T}_n}\cdot\nabla\phi(x)\,dx,$$

so that finally, using Corollary 4.11, we can pass to the limit in (61) and obtain

$$\int_\Omega\frac{\mathbf{K}}{\mu}(\nabla p-\rho\mathbf{g})\cdot\nabla\phi\,dx+\int_\Sigma\frac{\mathbf{K}_{f,\boldsymbol{\nu}}}{\mu}\left(\frac{[\![p]\!]}{b_f}-\rho\mathbf{g}\cdot\boldsymbol{\nu}\right)\frac{[\![\phi]\!]}{b_f}\,b_f\,ds-\int_\Sigma\overline{\phi}\Psi\,ds=\int_\Omega Q\phi\,dx.$$

Taking $\phi\in\mathcal{C}_c^\infty(\Omega)$ in this formulation, we get that p solves

$$\nabla\cdot\mathbf{v}^p=Q\text{ in }\Omega,$$

with $\mathbf{v}^p=-\frac{\mathbf{K}}{\mu}(\nabla p-\rho\mathbf{g})$. In particular $\mathbf{v}^p\in H_{\mathrm{div}}(\Omega)$ and comparing the Stokes formula (15) we get

$$\begin{cases}\mathbf{v}^p\cdot\mathbf{n}=0,\quad\text{on }\Gamma,\\ \Psi=[\![\mathbf{v}^p\cdot\boldsymbol{\nu}]\!],\\ \overline{\mathbf{v}^p\cdot\boldsymbol{\nu}}=-\dfrac{\mathbf{K}_{f,\boldsymbol{\tau}}}{\mu}\left(\dfrac{[\![p]\!]}{b_f}-\rho\mathbf{g}\cdot\boldsymbol{\nu}\right),\end{cases}$$

and then by (58), we find that the fracture pressure solves

$$p_f=\overline{p}-\frac{(2\xi-1)\mu}{4\mathbf{K}_{f,\boldsymbol{\nu}}}b_f[\![\mathbf{v}^p\cdot\boldsymbol{\nu}]\!],$$

that is $p_f=\Pi_f p$. Finally, replacing the above value for Ψ in (60), we recover the Darcy equation in the fracture and the claim is proved.

- **The case $\xi=\frac{1}{2}$**

  Note that, in that case, we can easily pass to the limit in (39) to find that

$$p_f=\frac{1}{2}(\gamma^+p+\gamma^-p)=\Pi_f p.\quad(62)$$

Unfortunately we do not have now any *a priori* bound on $[\![\mathbf{v}^{p^{\mathcal{T}_n}} \cdot \boldsymbol{\nu}]\!]$. Hence, we are not able to perform the limit independently in (43) and (44) as before. That is the reason why we are going to treat simultaneously the continuity equation in the porous matrix and in the fracture by passing to the limit in the global formulation (45) (the last term being 0 since $\xi = \frac{1}{2}$).

Taking here also $\phi^{\mathcal{T}_n} = \Pi^{\mathcal{T}_n,c}\phi$ for any $\phi \in \mathcal{S}$ in this formula, we get

$$\sum_{\mathcal{D}\in\mathfrak{D}} \int_{\mathcal{D}} \frac{\mathbf{K}}{\mu} \left(\nabla^{\mathfrak{M}_n,p^D} p^{\mathcal{T}_n} - \rho \Pi^{\mathfrak{D}_n}\mathbf{g}\right) \cdot \left((\nabla\phi(x)\cdot\mathbf{n}_\sigma + \widetilde{R}_n(x))\,\mathbf{n}_\sigma\right) dx$$
$$+ \int_\Sigma \frac{\mathbf{K}_{f,\boldsymbol{\tau}}}{\mu} (\nabla^{\mathfrak{S}_n}\Pi^{\mathfrak{S}_n} p^{\mathcal{T}_n} - \rho\mathbf{g}\cdot\boldsymbol{\tau})(\nabla_{\boldsymbol{\tau}}\overline{\phi}(s) + R_n(s)) b_f(s)\, ds$$
$$+ \int_\Sigma \frac{\mathbf{K}_{f,\boldsymbol{\nu}}}{\mu} \left(\frac{[\![p^{\mathcal{T}_n}]\!]}{b_{f,\sigma}} - \rho\mathbf{g}\cdot\boldsymbol{\tau}\right) \left(\frac{[\![\phi]\!] + r_n^+ - r_n^-}{b_{f,\sigma}}\right) b_f\, ds$$
$$= \int_\Omega Q(x)\Pi^{\mathfrak{M}_n,c}\phi\, dx + \int_\Sigma Q_f(s)(\overline{\phi}(s) + r_n(s)) b_f(s)\, ds,$$

By the same arguments than above, we can pass to the limit in this formula and obtain

$$\int_\Omega \frac{\mathbf{K}}{\mu}(\nabla p - \rho\mathbf{g})\cdot\nabla\phi\, dx + \int_\Sigma \frac{\mathbf{K}_{f,\boldsymbol{\tau}}}{\mu}(\nabla_{\boldsymbol{\tau}}\Pi_f p - \rho\mathbf{g}\cdot\boldsymbol{\tau})\nabla_{\boldsymbol{\tau}}\overline{\phi}(s) b_f(s)\, ds$$
$$+ \int_\Sigma \frac{\mathbf{K}_{f,\boldsymbol{\nu}}}{\mu}\left(\frac{[\![p]\!]}{b_f} - \rho\mathbf{g}\cdot\boldsymbol{\nu}\right)\frac{[\![\phi]\!]}{b_f} b_f\, ds = \int_\Omega Q\phi\, dx + \int_\Sigma Q_f\overline{\phi} b_f\, ds. \quad (63)$$

Taking first $\phi \in \mathcal{C}^\infty(\overline{\Omega})$ vanishing in a neighborhood of the fracture Σ, we see that $\nabla\cdot\mathbf{v}^p = Q$ in Ω and that the Neumann boundary condition (21) is satisfied.

Furthermore, we know from the compactness Lemma 4.12 that $\Pi_f p \in H^1(\Sigma)$, that is to say $\Pi_f p = \overline{p} \in H^1(\Sigma)$ by (62). It follows that p lies in the space $\mathcal{W}$ defined in section 3.1.2.

We use now the Stokes formula (15) for $\mathbf{v}^p$ and any $\phi \in \mathcal{S}$ and we compare to (63). It follows:

$$\left\langle [\![\mathbf{v}^p\cdot\boldsymbol{\nu}]\!], \overline{\phi}\right\rangle_{(H^{\frac12})',H^{\frac12}} + \left\langle \overline{\mathbf{v}^p\cdot\boldsymbol{\nu}}, [\![\phi]\!]\right\rangle_{H^{-\frac12},H^{\frac12}_{00}}$$
$$+ \int_\Sigma \frac{\mathbf{K}_{f,\boldsymbol{\tau}}}{\mu}(\nabla_{\boldsymbol{\tau}}\overline{p} - \rho\mathbf{g}\cdot\boldsymbol{\tau})\nabla_{\boldsymbol{\tau}}\overline{\phi}\, b_f(s)\, ds + \int_\Sigma \frac{\mathbf{K}_{f,\boldsymbol{\nu}}}{\mu}\left(\frac{[\![p]\!]}{b_f} - \rho\mathbf{g}\cdot\boldsymbol{\tau}\right)\frac{[\![\phi]\!]}{b_f} b_f\, ds = \int_\Sigma Q_f\overline{\phi} b_f\, ds. \quad (64)$$

For any $\psi \in \mathcal{C}_c^\infty(\Sigma)$, we easily build a function $\phi \in \mathcal{S}$ such that $\gamma^+\phi = \psi/2$ and $\gamma^-\phi = -\psi/2$, so that $\overline{\phi} = 0$ and $[\![\phi]\!] = \psi$. Using this particular test function in (64) for any such ψ, we deduce that

$$\overline{\mathbf{v}^p\cdot\boldsymbol{\nu}} = -\frac{\mathbf{K}_{f,\boldsymbol{\nu}}}{\mu}\left(\frac{[\![p]\!]}{b_f} - \rho\mathbf{g}\cdot\boldsymbol{\nu}\right).$$

Coming back to (64) and using now a test function ϕ such that $[\![\phi]\!] = 0$ we finally find that the continuity equation (22) and the boundary condition (23) are satisfied in the fracture Σ.

- **Conclusion**

  We proved the existence of a solution of the problem (19)-(23) for all $\xi \geq \frac12$. Furthermore, this problem admits at most one solution as shown in the previous section. Hence, we conclude that the whole sequence $(p^{\mathcal{T}_n})_n$ converges towards the unique solution of problem (19)-(23) in the sense given in the statement of the theorem.

■

5. Numerical results for some immersed polygonal fractures

We present numerical results for a computational domain $\Omega = [0,1]^2$. Let us recall that the permeability tensor is isotropic in the porous matrix - we choose $\mathbf{K} = \mathrm{Id}$ - and diagonal in the curvilinear frame of the fractures. We have taken in this section $\mathbf{g} = 0$, $\rho = \mu = 1$ and $Q = 0$, $Q_f = 0$, so that the flow is only generated by the boundary conditions.

We always take the quadrature parameter ξ equal to $\frac{1}{2}$, excepted in Section 5.3 where the influence of this parameter is investigated.

All the numerical results for both the asymptotic and the global Darcy models are presented when the mesh convergence is reached. We represent the distribution of the pressure field inside the domain from dark (high pressure values) to light (low pressure values). We also represent some of the streamlines of each flow.

5.1. The DDFV scheme for the global model

The difficulties in approximating by finite volume methods the *two-permeabilities* global Darcy model are twofold. The first one comes from the very different scales in the flow (the small aperture of the fractures, the high permeability ratios, ...). The second one comes from the anisotropy of the equation inside the fracture which requires a "gradient reconstruction" method to approximate fluxes across the edges; we choose a *Discrete Duality Finite Volume* approach (see [2], [10]). In presence of strong discontinuities of the permeability tensor, these DDFV schemes still converges but slowly (at rate 1/2). To recover a first order scheme, it is proposed and analysed in [9, 16] a *modified DDFV scheme*. This m-DDFV scheme ensures the local continuity and conservativity of the numerical fluxes across any edge of the mesh and is proved to be of first order in the discrete H^1-norm, even in presence of high permeablility jumps.

5.2. Results for a straight half-fracture with constant aperture

We consider the half fracture $\Sigma \times \left[-\frac{b_f}{2}, \frac{b_f}{2}\right]$, with $\Sigma = \{(x,y) \text{ such that } x = 0.5, y \geq 0.5\}$ and b_f is constant and equal to 0.01. Let us describe the various configurations and boundary conditions we propose to illustrate various typical flows and the behavior of the model under study in each case.

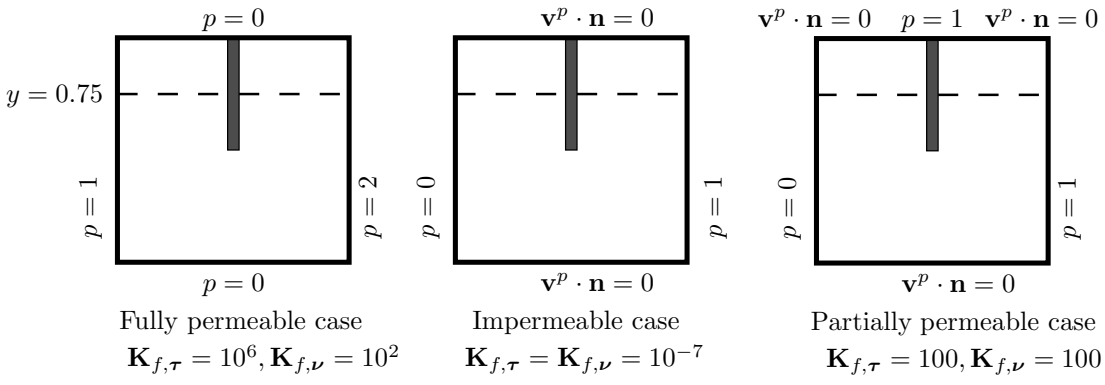

Figure 4. Configurations and boundary conditions for a straight half fracture

- **Fully permeable fracture, see Figure 4 (left).**

  The quantities $b_f \mathbf{K}_{f,\boldsymbol{\tau}}$ and $\dfrac{\mathbf{K}_{f,\boldsymbol{\nu}}}{b_f}$ are of the same order *e.g.* $\mathbf{K}_{f,\boldsymbol{\tau}} = 10^6$, $\mathbf{K}_{f,\boldsymbol{\nu}} = 100$. We impose Dirichlet boundary conditions on $\partial\Omega$: $p(\cdot,0) = 0, p(\cdot,1) = 0, p(0,\cdot) = 1, p(1,\cdot) = 2$.

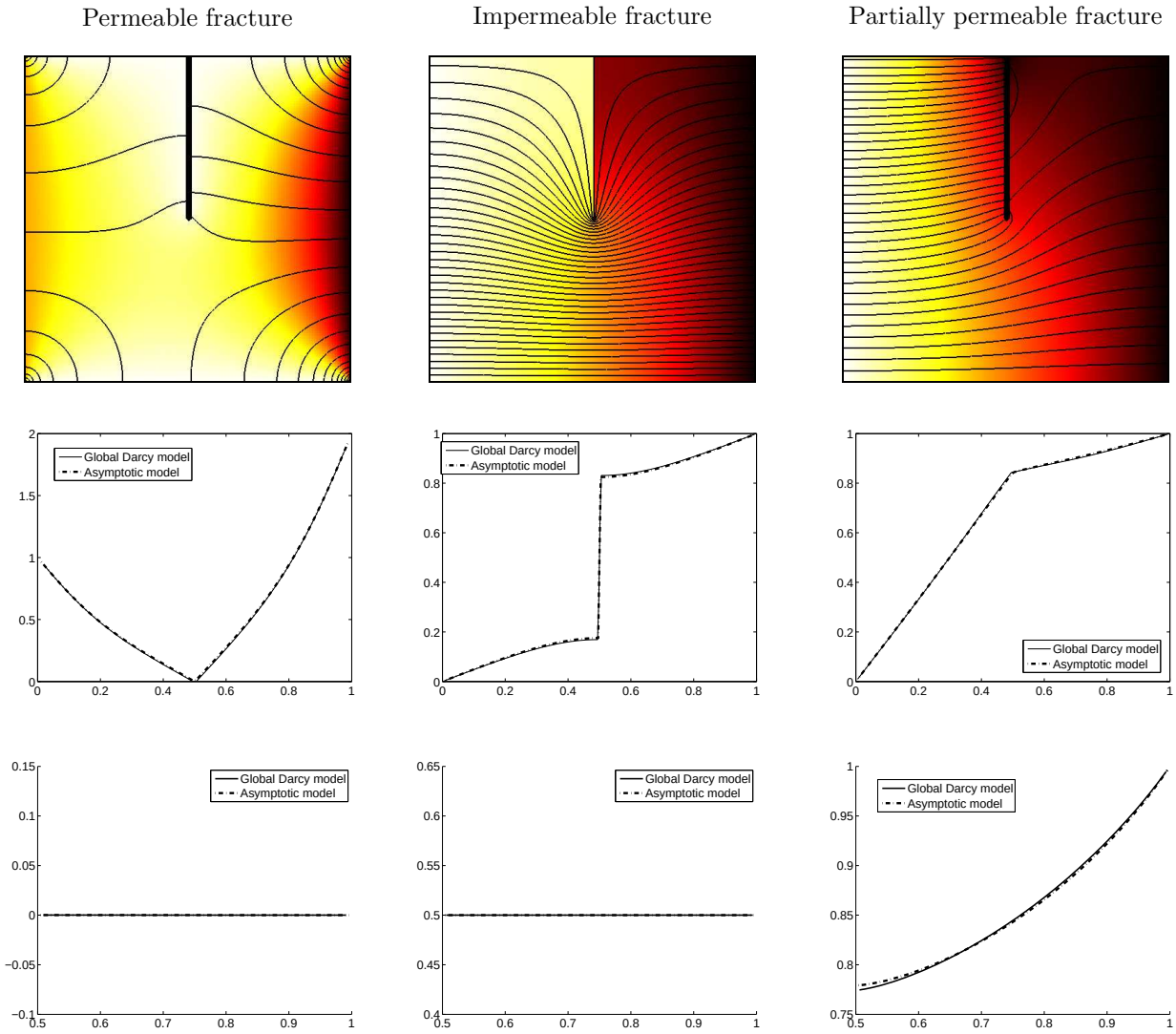

FIGURE 5. Pressure field and streamlines (top), Pressure along the cutline $y = 0.75$ (middle), Pressure along the fracture (bottom)

- **Impermeable fracture, see Figure 4 (center).**
  The quantity $b_f \mathbf{K}_{f,\boldsymbol{\tau}}$ is close to zero and $\dfrac{\mathbf{K}_{f,\boldsymbol{\nu}}}{b_f}$ remains small *e.g.* $\mathbf{K}_{f,\boldsymbol{\tau}} = 10^{-7}$, $\mathbf{K}_{f,\boldsymbol{\nu}} = 10^{-7}$. We impose mixed boundary conditions on $\partial\Omega$: $\mathbf{v}^p \cdot \mathbf{n}(\cdot, 0) = 0, \mathbf{v}^p \cdot \mathbf{n}(\cdot, 1) = 0, p(0, y) = 0, p(1, \cdot) = 1$.
- **Fracture with intermediate properties, see Figure 4 (right).**
  In this test, formally performed for the corresponding non-immersed fracture in [17, 18], the ratio between $\mathbf{K}_{f,\boldsymbol{\nu}}/b_f$ and $\mathbf{K}$ is high whereas $b_f \mathbf{K}_{f,\boldsymbol{\tau}}$ and $\mathbf{K}$ are of same order *e.g.* $\mathbf{K}_{f,\boldsymbol{\tau}} = 100$, $\mathbf{K}_{f,\boldsymbol{\nu}} = 100$.
  We impose mixed boundary conditions on $\partial\Omega$: $p(0, \cdot) = 0$, $p(1, \cdot) = 1$, $\mathbf{v}^p \cdot \mathbf{n}(\cdot, 0) = 0$, $\mathbf{v}^p \cdot \mathbf{n}(x, 1) = 0$ for any $x \neq \frac{1}{2}$, and $p(\frac{1}{2}, 1) = 1$.

In Figure 5, the results obtained by the resolution of the global Darcy two-permeabilities model by the m-DDFV methos and the resolution of the asymptotic model are compared. At the top part of the figure, we show the pressure field and some streamlines indicating the shape of the flow we are looking at in each case. In the middle part of the figure, we show the pressure on the horizontal cutline $y = 0.75$ whereas in the bottom part we show the pressure field along the fracture. In any cases, the curves for the global Darcy model and the asymptotic models are nearly identical.

These results show the ability of the asymptotic model to simulate efficiently all kinds of flows in fractured porous media, from impermeable fractures (where pressure jumps hold across the fracture) to fully permeable ones (where mass fluxes jumps hold across the fracture). The gain in using the asymptotic model is especially obvious for large permeability ratios or very anisotropic fracture permeabilies: the resolution of the global Darcy model typically requires six times more degrees of freedom than the asymptotic one in order to achieve mesh convergence of the numerical solutions for a given tolerance.

5.3. **Influence of the quadrature parameter ξ**

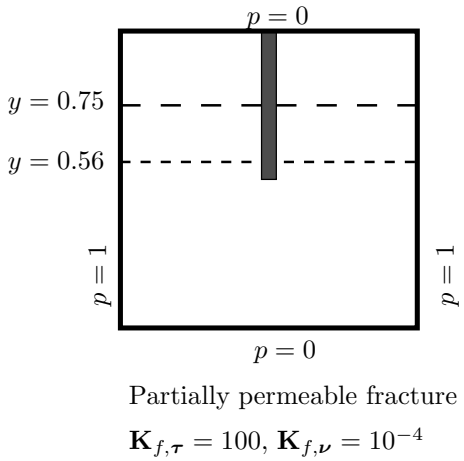

FIGURE 6. Boundary condition for a partially permeable fracture

In many situations, we observed that the influence of the quadrature parameter ξ is almost negligible and any value in the interval $[1/2, 1]$ gives satisfactory results. Nevertheless, the influence of the parameter ξ can be observed in some cases. We choose here for instance a fracture with a very high anisotropy $\mathbf{K}_{f,\boldsymbol{\tau}} = 100$, $\mathbf{K}_{f,\boldsymbol{\nu}} = 10^{-4}$. We consider Dirichlet boundary conditions for the pressure: $p = 1$ on the vertical sides and $p = 0$ on the horizontal ones (see Figure 6).

In Figure 7, we show the pressure field obtained with the global Darcy model on a mesh with 65560 control volumes (that is the reference solution) and the solutions obtained for various values of ξ for the asymptotic model on a mesh with 16384 control volumes. We see that $\xi = 1/2$ seems to give a sharper solution than the one for $\xi = 3/4$ which is used by some authors. We also point out that for $\xi < 1/2$, the asymptotic model can become ill-posed or unstable (in the present situation, negative values of the pressure appear).

In Figure 8, we go further in the comparisons by showing, on the left part of the figure, the pressure obtained along the fracture in each case. More precisely, we plot $\Pi_f p(s)$ for the two models $\xi = 1/2$ and $\xi = 3/4$, as well as the quantity $\bar{p}(s) = (\gamma^+ p(s) + \gamma^- p(s))/2$ for $\xi = \frac{3}{4}$. We recall that when $\xi = 1/2$, we have $\Pi_f p = \bar{p}$ that is the reason why there is only one curve in that case.

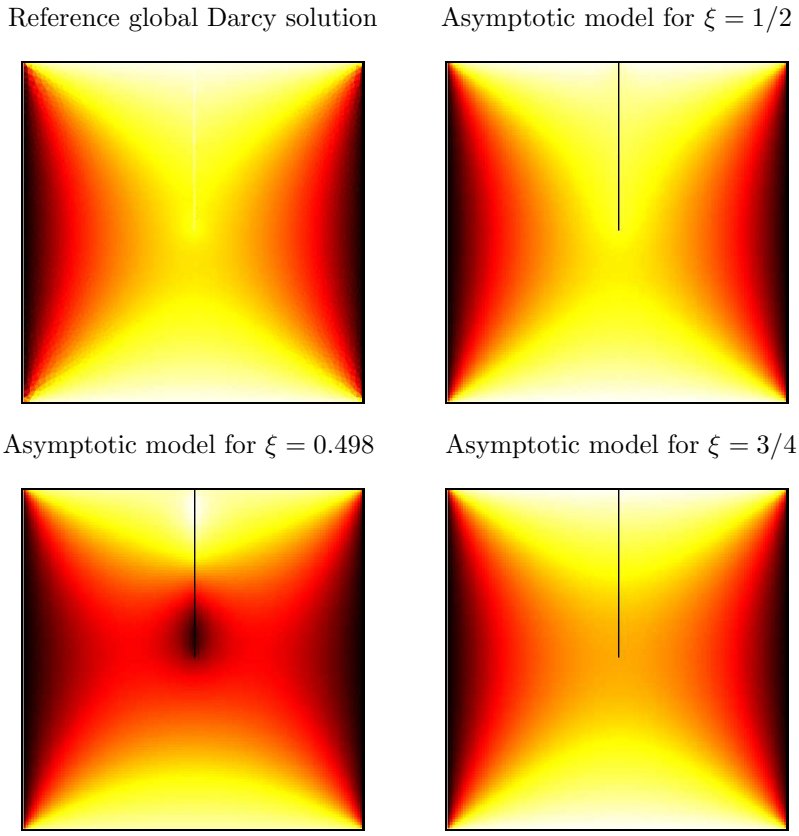

FIGURE 7. Comparison between the pressure field obtained with the global Darcy model and the asymptotic model for various values of ξ

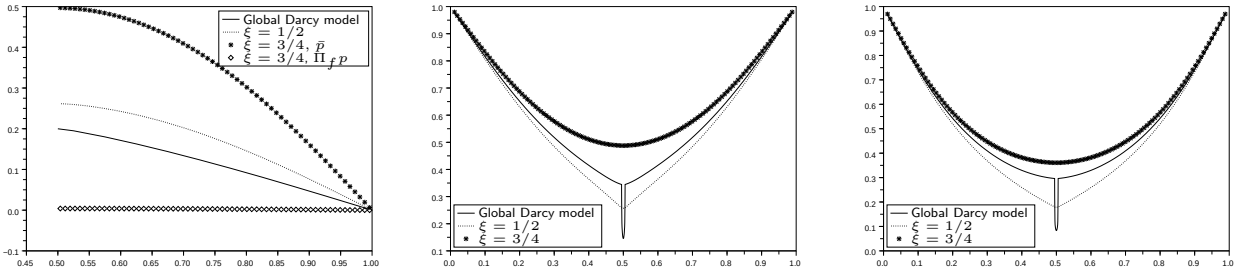

FIGURE 8. Comparison of pressure along and across the fracture between the global Darcy model and the asymptotic model for $\xi = 0.5$ and $\xi = 0.75$

The reference mean-pressure $s \mapsto \frac{1}{b_f} \int_{-b_f/2}^{b_f/2} p(t,s)\, dt$ computed by the resolution of the global Darcy model on the fine grid is also given for reference. These results confirm that the model for $\xi = \frac{1}{2}$ leads to more precise results.

The other two parts (center and right) of Figure 8 show the pressure along two cutlines $y = 0.5625$ and $y = 0.75$. It is confirmed that the model for $\xi = \frac{3}{4}$ badly computes the pressure inside the fracture, but is quite satisfactory outside the fracture, at least far enough from the extremity of Σ fully immersed in $\tilde{\Omega}$.

As a conclusion, in the remaining of this paper, we systematically use the value $\xi = 1/2$ in our computations.

5.4. **Results for a network of half straight fractures**

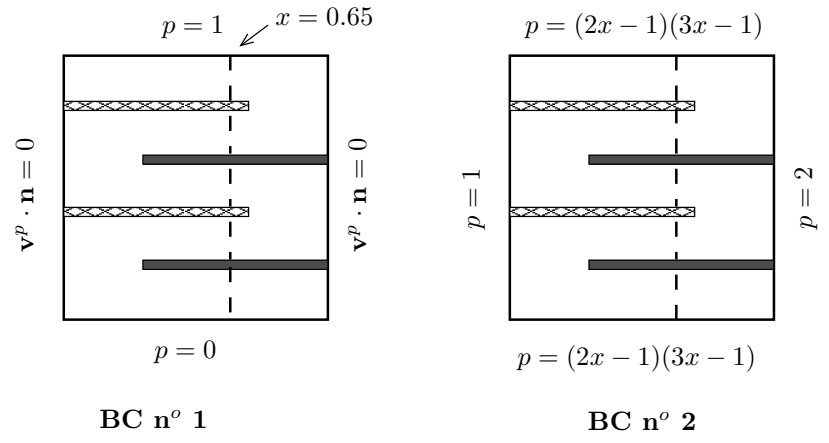

FIGURE 9. Configuration and boundary conditions for a network of half straight fractures

We consider here a set of four horizontal fractures of aperture $b_f = 0.01$ defined by $\mathcal{F}_i = \Sigma_i \times \left[-\frac{b_f}{2}, \frac{b_f}{2}\right]$, with $\Sigma_1 = \{(x, y) \text{ such that } x \geq 0.3, y = 0.2\}$, $\Sigma_2 = \{(x, y) \text{ such that } x \leq 0.7, y = 0.4\}$, $\Sigma_3 = \{(x, y) \text{ such that } x \geq 0.3, y = 0.6\}$, $\Sigma_4 = \{(x, y) \text{ such that } x \leq 0.7, y = 0.8\}$. The fractures $\mathcal{F}_2$ and $\mathcal{F}_4$ are impermeable $\mathbf{K}_{f,\boldsymbol{\tau}} = \mathbf{K}_{f,\boldsymbol{\nu}} = 10^{-2}$, whereas $\mathcal{F}_1$ and $\mathcal{F}_3$ present intermediate properties $\mathbf{K}_{f,\boldsymbol{\tau}} \in \{1, 10\}$ and $\mathbf{K}_{f,\boldsymbol{\nu}} = 10^{-2}$. For the boundary conditions described in Figure 9, we compare in Figure 10 the solution (solid line) of the global Darcy model using a mesh with 68160 control volumes, and the solution (dashed line) of a the asymptotic model, using a mesh with 25600 control volumes, along the four fractures Σ_i and along the cutline $\{x = 0.65\}$.

We observe a perfect agreement of the two solutions in the first two cases since the curves are almost indistinguishable. In the third case, where $\mathbf{K}_{f,\boldsymbol{\tau}}$ is larger, we can see that we approach the validity limit of the model. It appears that the Neuman boundary condition at the boundary of the fracture is not perfectly suitable in this case. A more precise modelling of the asymptotic boundary condition on $\partial\Sigma$ seems to really be necessary in this kind of situations.

5.5. **Fracture with variable aperture**

We now investigate the ability of the asymptotic model to simulate flows in fractures with variable aperture. We consider (see Figure 11) a vertical conic-shaped fracture at $x = \frac{1}{2}$ where b_f varies linearly from 0.001 (bottom) to 0.019 (top). We consider an isotropic case $\mathbf{K}_{f,\boldsymbol{\tau}} = \mathbf{K}_{f,\boldsymbol{\nu}} = 100$.

In Figure 12, we compare the results obtained by the global Darcy model (left part of the figure) and by the asymptotic model (center part of the figure). We can see a quite good agreement. Notice that the mesh used to compute the global Darcy solution has to be very fine near the bottom of the fracture since its aperture is equal to 10^{-3} in this area. More precisely, the asymptotic results presented here have been obtained for a rectangular mesh with 16000 control volumes, whereas the global Darcy computation has been performed on a triangular mesh with 100000 control volumes, suitably refined in the neighbourhood of the fracture.

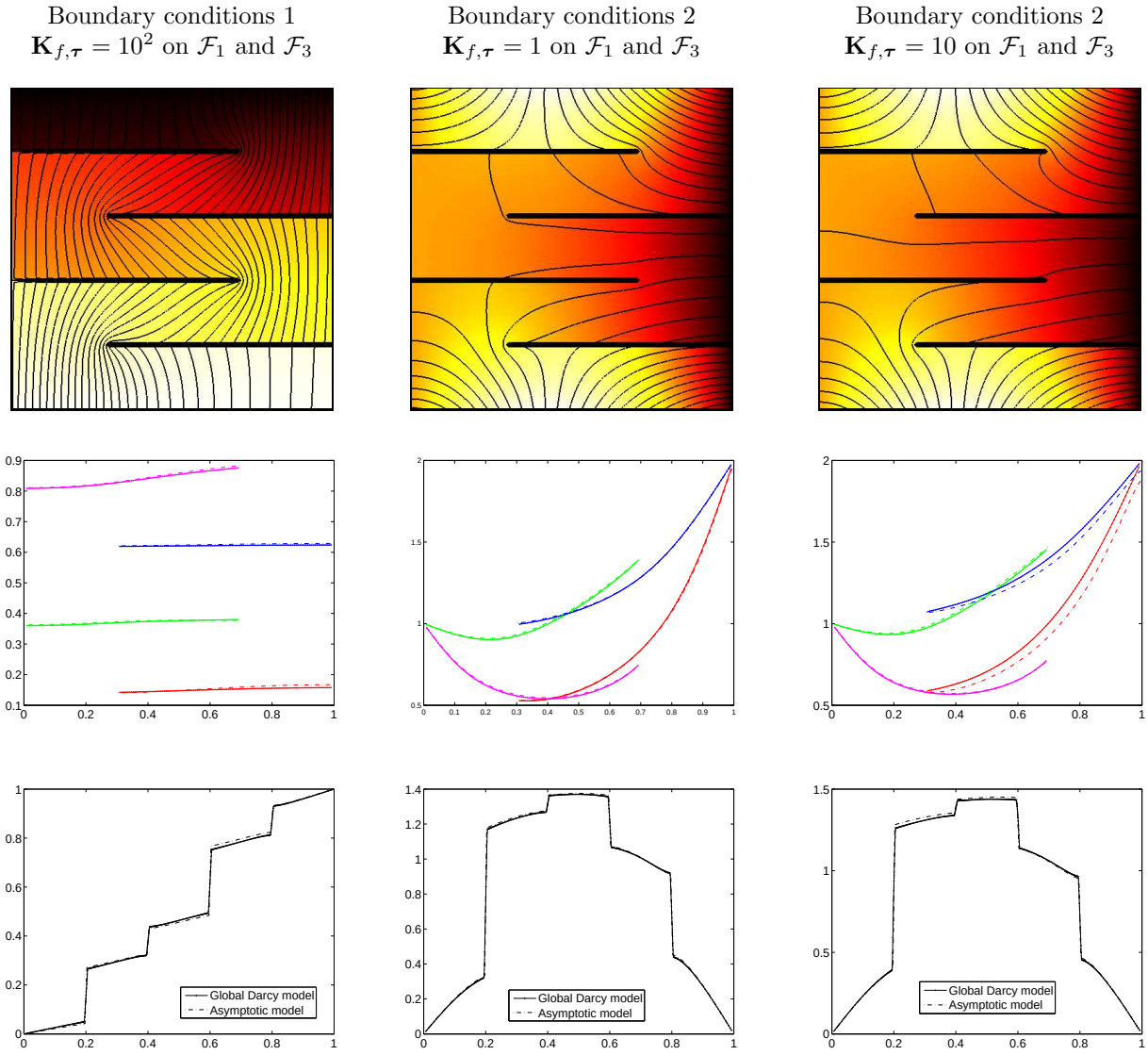

FIGURE 10. Pressure field and streamlines (top), Pressure along the four fractures (middle), Pressure along the cross section $\Sigma_\perp$ (bottom)

We also give for comparison, the result obtained with the asymptotic model if we replace the variable (linear) aperture $b_f(s)$ with a constant mean-value $b_f(s) \equiv 10^{-2}$, which amounts to approximate the conic-shaped fracture with an "equivalent" constant aperture fracture. We clearly see that the result is unsatisfactory which demonstrates the necessity to suitably take into account the geometry of the fracture in the asymptotic model.

5.6. **Comparison with an analytic solution**

We finally test the model in the case of a permeable lens-shaped fracture, using the analytic behaviour of the flow obtained in [19] in the neighbourhood of the extremities of the lens embedded in an infinite porous medium. This lens, centered in $(0.5, 0.5)$ and whose length is 0.2, is limited by two parts of circles of same

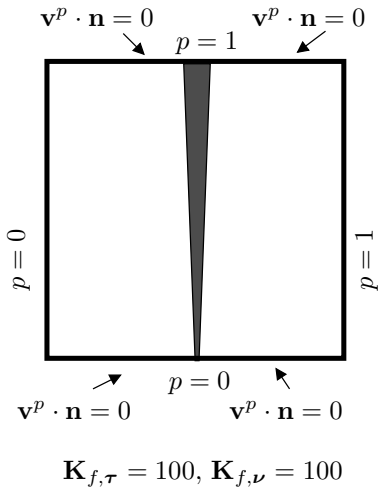

FIGURE 11. Configuration and boundary conditions for the conic-shaped fracture

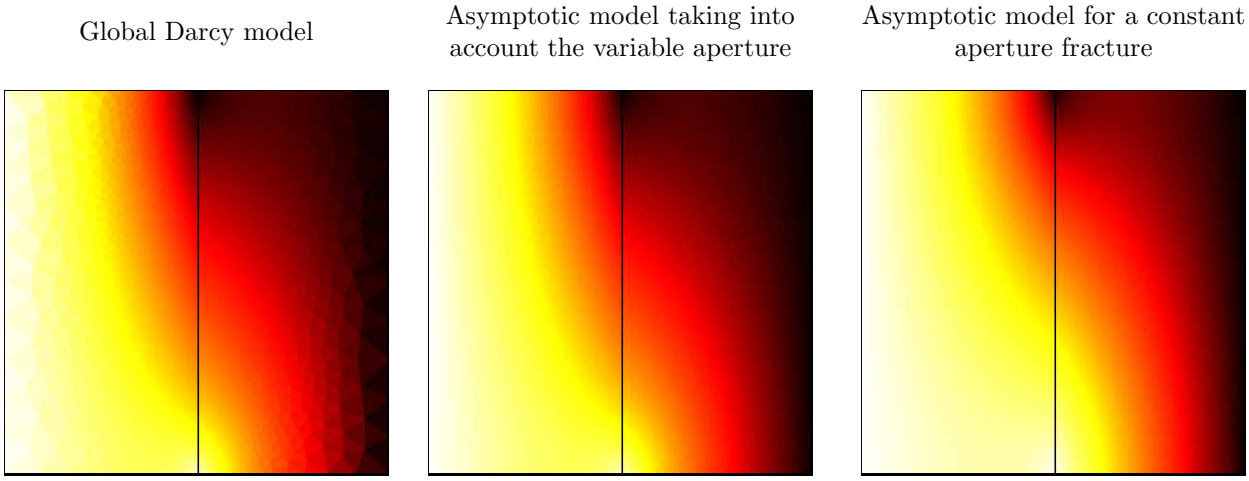

FIGURE 12. Influence of the shape of the fracture

radius meeting with a right angle. We refer to Figure 13 which also presents the boundary conditions used for the numerical simulations. We consider the isotropic case where $\mathbf{K}_{f,\boldsymbol{\tau}} = \mathbf{K}_{f,\boldsymbol{\nu}} = K_f = 12$. For a flow parallel to the main symmetry axis of the lens, the analytic solution derived in [19] in the neighbourhood of the extremity $(0.5, 0.6)$, is equivalent up to a constant to

$$p^{\text{anal}}(y) \sim \begin{cases} \frac{4}{(K_f+1)\Delta} \left(\frac{0.6-y}{y-0.4}\right)^{\gamma_1}, & y < 0.6, \\ \frac{2}{\Delta} \left(\cos(\pi\gamma_1) - \frac{K_f-1}{K_f+1} \cos\left(\frac{\pi\gamma_1}{2}\right)\right) \left(\frac{y-0.6}{y-0.4}\right)^{\gamma_1}, & y \geq 0.6, \end{cases}$$

with $\Delta = \cos(\pi\gamma_1) - \frac{1}{2}\frac{K_f-1}{K_f+1} \cos\left(\frac{\pi\gamma_1}{2}\right)$, $\gamma_1 = \frac{2}{\pi}\text{acos}\left(\frac{1}{2}\frac{K_f-1}{K_f+1}\right)$.

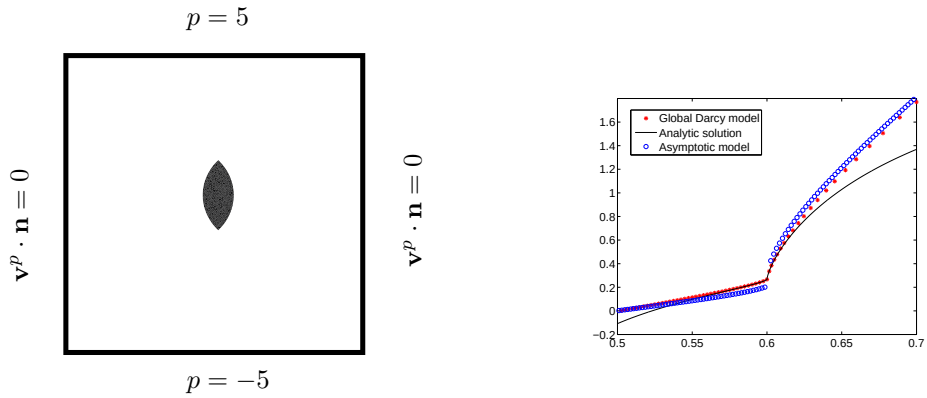

FIGURE 13. The lens-shaped fracture : Configuration and boundary conditions (left), Pressure field along the symmetry axis $x = 0.5$ of the fracture near one of its extremity (right).

The right part of Figure 13 shows the good agreement near the extremity between this analytic solution and the global Darcy solution, computed on a triangular mesh with 20000 cells. Note that we chose for the additive constant the pressure value given by the global Darcy solution at the angular point $(0.5, 0.6)$. The solution given by the asymptotic model on a mesh composed by 13000 triangles is globally close to the global Darcy solution, except in the very neighbourhood of the extremity of the lens, where the aperture b_f vanishes. Since the aperture ($\mathbf{s}$) vanishes at the two extremities of the fracture, this test case does not enter the analysis proposed in this paper. Nevertheless, the model seems to give satisfactory results event in this situation.

6. Conclusion and perspectives

In this study, some asymptotic models of flow in fractured porous media are formally derived in the case where the fracture domains, whose aperture is supposed to be small, are reduced to polygonal interfaces immersed inside the porous matrix. It is then needed to solve an adequate 1D Darcy-type equation along these immersed interfaces, coupled with an usual 2D Darcy equation in the porous matrix.

A cell-centered Finite Volumes scheme is investigated to solve this coupled problem. Existence of solutions to the asymptotic models is stated by passing to the limit into the FV scheme, whereas uniqueness is ensured by energy estimates. The convergence proof of the scheme is quite intricate due to the fact that, because of the immersed interfaces, the domain under study is no more located on one side of its boundary.

Using the proposed numerical scheme, the behavior and the validity of the asymptotic models under study are then investigated for a large variety of situations. On these examples, we obtain a good agreement with the solutions computed analytically or obtained by using apropriate numerical schemes for the global Darcy problem on locally refined meshes. In our experiments, the number of required degrees of freedom saved with the use of the asymptotic models proves to be all the more important than the permeability jumps are large.

Showing that, in the case of fully immerged fractures, the solution of the asymptotic model proposed here is actually a correct approximation of the solution of the global Darcy model in the limit $\to \mathbf{0}$ is devoted to a further work. It would be interesting to investigate the coupling of such models with a time dependent advection-diffusion equation for the solutal transport in order to study solutal dispersion phenomena in fractured porous media. Another perspective can be to consider fractures in which the flow is governed by the Stokes equation instead of the Darcy one.

Acknowledgements

The authors want to thank P. Adler for many stimulating discussions. This study has been carried out in the framework of the research project "Dispersion in fractured porous media" which received a financial support from the GdR CNRS MoMaS in the period 2004–2006.

References

[1] Adler P.M., Thovert J.-F., Fractures and Fracture Networks, *K*luwer Acad., Amsterdam, 1999.
[2] Andreianov B., Boyer F. and Hubert F., Discrete duality finite volume schemes for Leray-Lions type elliptic problems on general 2D-meshes, Num. Meth. for PDEs, Vol. 23, N°1, pp 145–195, 2007.
[3] Angot P., Finite volume methods for non smooth solution of diffusion models; application to imperfect contact problems, in *Recent Advances in Numerical Methods and Applications*, Proc. 4th Int. Conf. NMA'98, Sofia (Bulgarie), O.P. Iliev, M.S. Kaschiev, S.D. Margenov, Bl.H. Sendov, P.S. Vassilevski (Eds.), pp. 621-629, World Sci. Pub, 1999.
[4] Angot P., Gallouët T., Herbin R., Convergence of finite volume methods on general meshes for non smooth solution of elliptic problems with cracks, in *Finite Volumes for Complex Applications II*, R. Vilsmeier, F. Benkhaldoun and D. Hänel (Eds), pp. 215-222, Hermès, 1999.
[5] Angot P., A model of fracture for elliptic problems with flux and solution jumps, *C.* R. Acad. Sci. Paris, Ser. Math., **337** (6), pp. 425-430, 2003.
[6] Angot P., Cancès C., A new numerical model of solutal transport in fractured porous media, submitted.
[7] Bear J., Tsang C.-F., de Marsily G. (Eds), Flow and Contaminant Transport in Fractured Rock, *A*cademic Press, San Diego, 1993.
[8] Bogdanov I.I., Mourzenko V.V., Thovert J.-F., Adler P.M., "Effective permeability of fractured porous media in steady-state flow", Water Resour. Res., **107**, 2002.
[9] Boyer F., Hubert F., Finite volume method for 2D linear and non linear elliptic problems with discontinuities, `http://hal.archives-ouvertes.fr/hal-00110436`, 2006.
[10] Domelevo K., Omnes P., A finite volume method for the Laplace equation on almost arbitrary two-dimensional grids, M^2AN, **39** (6), pp. 1203-1249, 2005.
[11] Eymard R., Gallouët T., H-convergence and numerical schemes for elliptic equations, *S*IAM Journal on Numerical Analysis, **41** (2), 539-562, 2003.
[12] Eymard R., Gallouët T., Herbin R., Finite Volume Methods, in *Handbook of Numerical Analysis*, P.G. Ciarlet and J.L. Lions (Eds), Vol. VII, 713-1020, North-Holland, 2000.
[13] Faille I., Flauraud E., Nataf F., Pégaz-Fiornet S., Schneider F., Willien F., A new fault model in geological basin modelling. Application of finite volume scheme and domain decomposition methods, in *Finite Volumes for Complex Applications III*, R. Herbin and D. Kröner (Eds), pp. 543-550, Hermes Penton Sci. (HPS), 2002.
[14] Faybishenko B., Witherspoon P.A., Benson S.M. (Eds), Dynamics of Fluids in Fractured Rock, *G*eophysical Monograph Series, **122**, American Geophysical Union, Washington D.C, 2000.
[15] Grisvard, P., Elliptic problems in nonsmooth domains, *Monographs and Studies in Mathematics*, Vol. 24, Pitman (Advanced Publishing Program), Boston, 1985.
[16] Hermeline F., Approximation of diffusion operators with discontinuous tensor coefficients on distorted meshes, *C*omput. Methods Appl. Mech. Engrg., **192**, pp. 1939–1959, 2003.
[17] Jaffré J., Martin V., Roberts J.E., Generalized cell-centered finite volume methods for flow in porous media with faults, in *Finite Volumes for Complex Applications III*, R. Herbin and D. Kröner (Eds), pp. 357-364, Hermes Penton Sci. (HPS), 2002.
[18] Martin V., Jaffré J. , Roberts J.E., Modeling fractures and barriers as interfaces for flow in porous media, *SIAM J. Sci. Comput.*, **26** (5), pp. 1667–1691, 2005.
[19] Mityushev V., Adler P. M., Darcy flow arround a two dimensional lense, *Journal Phys. A: Math. Gen.*,**39**, pp. 3545–3560, 2006.